PHYSICAL REVIEW D **78,** 114017 (2008)

D-state effects in the electromagnetic $N\Delta$ transition

G. Ramalho,[1,2] M. T. Peña,[2,3] and Franz Gross[1,4]

[1]*Thomas Jefferson National Accelerator Facility, Newport News, Virginia 23606, USA*
[2]*Centro de Física Teórica de Partículas, Av. Rovisco Pais, 1049-001 Lisboa, Portugal*
[3]*Department of Physics, Instituto Superior Técnico, Av. Rovisco Pais, 1049-001 Lisboa, Portugal*
[4]*College of William and Mary, Williamsburg, Virginia 23185, USA*

(Received 23 October 2008; published 17 December 2008)

We consider here a manifestly covariant quark model of the nucleon and the Δ, where one quark is off shell, and the other two quarks form an on-shell diquark pair. Using this model, we have shown previously that the nucleon form factors and the dominant form factor for the $\gamma N \rightarrow \Delta$ transition (the magnetic dipole (M1) form factor) can be well described by nucleon and Δ wave functions with S-state components only. In this paper, we show that nonvanishing results for the small electric (E2) and Coulomb (C2) quadrupole form factors can be obtained if D-state components are added to the Δ valence quark wave function. We present a covariant definition of these components and compute their contributions to the form factors. We find that these components cannot, by themselves, describe the data. Explicit pion cloud contributions must also be added, and these contributions dominate both the E2 and the C2 form factors. By parametrizing the pion cloud contribution for the transition electric and Coulomb form factors in terms of the neutron electric form factor, we estimate that the contributions of the Δ D-state coupled to quark core spin of $3/2$ is of the order of 1%, and the contributions of the Δ D-state coupled to quark core spin $1/2$ is of the order of 4%.

DOI: 10.1103/PhysRevD.78.114017 PACS numbers: 12.39.Ki, 13.40.Gp, 11.30.Cp, 14.20.Gk

I. INTRODUCTION

Understanding the internal structure of the baryons is both an experimental and a theoretical challenge. Experimentally, the main source of information has been the electro- and photo- excitation of the nucleon, which allows to parametrize the baryons internal structure in terms of their electromagnetic form factors. Very accurate JLab data [1–3] exist nowadays for the nucleon elastic form factors. Also, theoretical models for the nucleon form factors are able to describe this data well [4–9]. The next step is the description of the nucleon excitations, starting with the Δ resonance. In recent years, new precise data have been collected from MAMI [10,11], LEGS [12], MIT-Bates [13], and JLab [14,15] in the region $Q^2 \leq 6$ GeV^2 ($q^2 = -Q^2$ is the squared momentum transfer). The $N\Delta$ electromagnetic transition ($\gamma N \rightarrow \Delta$) has a simple interpretation in terms of the valence quark structure: the Δ results from a spin flip of a single quark in the nucleon. It is then understandable that the magnetic dipole multipole M1 dominates the transition for low Q^2, and that the electric E2 and the Coulomb C2 quadrupoles give only small contributions, of the order of a few percent. For large Q^2 however, according to perturbative QCD (pQCD) [16,17], equally important contributions from M1 and E2 are to be expected, but the scale for the outset of that regime is not yet known exactly.

Several theoretical descriptions have been proposed for low, intermediate, as well as for the large transfer momentum Q^2 regions. These descriptions involve two ingredients: the valence quark and the nonvalence degrees of freedom. The nonvalence degrees of freedom are essentially the sea quark contributions, which represent quark-antiquark states, and are usually called meson cloud effects. Because of its pseudoscalar character and its low mass, chiral symmetry assigns a special role to the pion [18,19], and pion cloud effects are therefore expected to contribute significantly to the baryon excitations. At low momentum transfer effective field theory (EFT) models based on chiral symmetry and perturbation theory (χPT) [20–23], with nucleon, Δ and pion degrees of freedom, and no internal structure considered, work well. EFTs describe the pion cloud effects at low momenta, but have a limited range of application, $Q^2 < 0.25$ GeV^2. At low Q^2, the large N_c limit [24,25] can be used to establish the main Q^2 dependence of the form factors and derive relations between the nucleon and the $N\Delta$ form factors [24]. At large Q^2, models within pQCD [16,26] with quarks and gluons as degrees of the freedom, can be applied. As for the intermediate momentum region, it may be appropriately featured by constituent quarks models [19,27–40], and models based on hadronic degrees of freedom, as the so-called dynamical models (DM) [41–46]. Quark models with mixed coupling with pion fields have also been proposed [19,27,47–54]. In the intermediate regime results from vector meson dominance models [55], QCD sum rules [56,57] and global parton distributions [58–60], have been presented as well. Finally, precise calculations are recently emerging from lattice QCD calculations [61–64]. For a review of the state-of-the-art in experiments and theory see Refs. [19,65–67].

There is at present a strong motivation to pursue an interplay between DM and constituent quark models

[19,27,43,66]. On one side, constituent quark models underestimate the result of the transition form factors, when not combined with explicit pion degrees of freedom [27,43,65,66,68]. On the other hand, dynamical models are based on sets of equations coupling electromagnetic excitations to meson (de)excitations of the baryons, and include pion cloud effects naturally and nonperturbatively. Examples are the Sato and Lee (SL) [41–43], the Dubna-Mainz-Taipei (DMT) [44,45] and the (dynamical) Utrecht-Ohio [46] models. Although very successful in the description of the $\gamma N \rightarrow \Delta$ form factors, they need to assume an initial parametrization for the baryon transition vertex, interpreted as the bare vertex, where no pion loop is taken. In a less ad hoc fashion, the bare vertex should therefore be derived from a quark model [66]. At the same time we can use the available models to extract the bare vertex. This is the goal of the EBAC program [43,66,69]. Alternative descriptions of the pion cloud and its relation to the deformations of the baryons were also proposed by Buchmann *et al.* [53,70–72]. For an updated review of the dynamical models see Refs. [43,73,74].

From the literature it is not clear which effects are due to the valence quarks, and which are related with the pion cloud, in particular, for the E2 and C2 multipoles. There is disagreement about those effects, between models based on different formalisms, such as the dynamical and EFT models, and even between models based on the same framework, as effective fields theories [74]. Also in the experimental sector there are some ambiguities. The form factors are extracted using multipole analysis based on unitary isobar models (UIMs) like MAID [75–77], SAID [78–81], or JLab/Yereven [82,83], each leading to different results due to the differences in parametrizations of the background and resonance structures, even considering dynamical models [41–46] instead of unitary isobar models [18,43,45,67]. The ambiguities involved in the interpretations of the data are well illustrated by the differences between the CLAS results [15] and the MAID analysis of the same data [75], and also the recent preliminary CLAS data analysis [43,67,84] based on different models. The results that we obtained here for G_C^* in particular, illustrate well the need to clarify these issues, as we will discuss later in this paper.

In a previous work [4,5,68] the spectator formalism [85–87] was applied to the nucleon and to the Δ baryons, considering only S-state wave functions. As shown in that work, with S-waves alone in the baryon wave functions, only the dominant of the three form factors for the $\gamma N \rightarrow \Delta$ transition does not vanish. Therefore, here we explore for the first time the effects of the D states in the Δ wave function within that formalism, and show here that those components in the Δ wave function lead to nonzero contributions for the subleading form factors E2 and C2. The origin of the D-wave states is well known: in the pioneering work of Isgur-Karl [28,65] the baryons are described as a system of confined quarks, where a tensor color hyperfine interaction is generated by one-gluon-exchange processes. This tensor interaction leads to SU(6) symmetry breaking, and allows the transition from the ground S state to an excited D state.

For each of the three $N\Delta$ electromagnetic transition form factors, we identified and separated the roles from the different partial wave components. While the magnetic dipole form factor G_M^*, the dominant contribution, is mainly due to the transition between the nucleon and the S state of the Δ, the electric quadrupole form factor G_E^* proceeds through the transition to a D state of the Δ corresponding to a three-quark core spin of $3/2$. Finally, the Coulomb quadrupole form factor G_C^* becomes nonzero, only when the transition to a D state of the Δ corresponding to a three-quark core spin $1/2$ is switched on. Nevertheless, and in agreement with other quark models, we conclude that the valence quark effects are not sufficient to describe the E2 and C2 data [19,20,27].

Additional mechanisms involving the sea quark states, mainly the pion cloud effects, are needed to fill the gap between the theory and the experimental data. The systematic and consistent treatment of the pion cloud mechanisms is out of the scope of this work, which is focused on the D-state effects, but is planned for a future work. In order to estimate the magnitude of the D states we considered the simple parametrization of the pion cloud in terms of the nucleon (neutron) electric form factor, with no additional parameters. This parametrization was derived from the basic properties of the quark models [large N_c limit and also SU(6) symmetry breaking] and is limited in its range of application to low Q^2. Nevertheless, we need to include a pion cloud parametrization for a realistic estimate of the weight of the D-wave components in the Δ wave function.

This paper is organized as follows: the formalism for the D-wave components of the Δ wave function is explained in Sec. II, the definitions of the form factors and other general results are introduced in Sec. III, the issue of gauge invariance and how it couples to the orthogonality of the initial and final state is dealt with in Sec. IV, the formulas for the form factors within the valence quark model used here are given in Sec. V. In Sec. VI, we discuss the contributions of the sea quarks (pion cloud), and in Sec. VII we present the numerical results for representative models based on valence and sea quarks. A discussion follows in Sec. VIII, and conclusions are presented in Sec. IX.

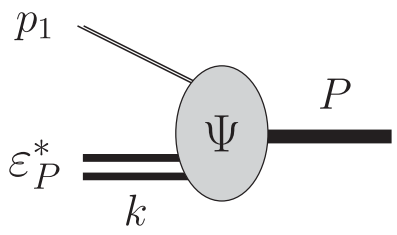

FIG. 1. Baryon quark-diquark wave function amplitude.

II. NUCLEON AND Δ WAVE FUNCTIONS

In the framework of the spectator theory [85,86] a baryon with four-momentum P is taken to be a bound state of a quark-diquark system, with relative four-momentum k, and is described by a covariant amplitude $\Psi(P, k)$. The diquark is taken to be on-mass-shell with an average mass m_s. The 3-quark wave function amplitude depicted in the diagram of Fig. 1 has S-wave components which, for the nucleon and the Δ, were already presented in Refs. [4,68]. Therefore, they will be only very briefly reviewed here, where the main focus is on the construction of D-wave components within the same underlying formalism. In the following, we will use H to denote either the nucleon (N), with mass $m_H = m_N = m$, or the Δ with mass $m_H = m_\Delta = M$.

The antisymmetry for the color part of the baryon wave function implies that, for S and D waves, the spin-isospin part of the wave function is symmetric. This in turn implies that the diquark has positive parity.

A. S-wave components of the nucleon and Δ wave functions

The S-wave part of the nucleon wave function has two components corresponding, respectively, to a diquark of spin 0-isospin 0 and a diquark of spin 1-isospin 1. Labeling the polarization of the spin-1 diquark by λ, these two terms for the nucleon amplitude shown in Fig. 1 can be written as

$$\Psi^S_{N\lambda_n}(P, k) = \frac{1}{\sqrt{2}}[\phi^0_I u_N(P, \lambda_n) - \phi^1_I \varepsilon^{\alpha *}_{\lambda P} U_\alpha(P, \lambda_n)] \times \psi^S_N(P, k). \tag{2.1}$$

The isospin states $\phi^{I_d}_I$ (with $I_d = 0$, 1 the diquark isospin) are, respectively, $\phi^0_I = \xi^{0*}\chi_I$ and $\phi^1_I = -\frac{1}{\sqrt{3}}(\tau \cdot \xi^{1*})\chi_I$, where ξ^{0*} is the diquark isospin-0 state and ξ^{1m*} are the Cartesian components of the isospin-1 state with projections $m = 0, \pm 1$, and χ_I is the nucleon isospin state with nucleon isospin projection $I = \pm 1/2$. As explained in Refs. [4,5], $(\tau \cdot \xi^{1*})\chi_I$ generates the 3-quark isospin state in terms of the nucleon isospin.

On the Dirac space, the the spin-0 component is simply $u_N(P, \lambda_n)$ (denoted simply by $u(P, \lambda_n)$ in our previous work), where λ_n is the projection of the nucleon spin along the z axis. The spin-1 component is a vector product of the diquark polarization vectors $\varepsilon^{\alpha *}_{\lambda P}$ and the Dirac operator

$$U_\alpha(P, \lambda_n) = \frac{1}{\sqrt{3}}\gamma_5\left(\gamma_\alpha - \frac{P_\alpha}{m_H}\right)u_N(P, \lambda_n), \tag{2.2}$$

with (generalizing the definition of u_N to u_H for an arbitrary hadron with mass m_H)

$$u_H(P, \lambda_H) = \sqrt{\frac{E_H(\mathrm{P}) + m_H}{2m_H}}\begin{bmatrix} 1 \\ \frac{2\lambda_H \mathrm{P}}{E_H(\mathrm{P}) + m_H} \end{bmatrix}\chi_{\lambda_H}, \tag{2.3}$$

where $E_H(\mathrm{P}) = \sqrt{m_H^2 + \mathrm{P}^2}$. Note that $u_H(P, \lambda_H)$ is independent of m_H when $\mathrm{P} = 0$.

Note also that $U_\alpha(P, \lambda_n)$ satisfies the two auxiliary conditions

$$(\not{P} - m)U_\alpha(P, \lambda_n) = 0 \qquad P^\alpha U_\alpha(P, \lambda_n) = 0. \tag{2.4}$$

The S-wave component of the Δ wave function must be symmetric in spin and isospin. Because the total isospin of the Δ is 3/2 the diquark spin 0-isospin 0 component cannot contribute, and the Δ wave function can contain only a diquark spin-1 isospin-1 component. As defined in Ref. [68], the S-wave component of the Δ wave function is written as

$$\Psi^S_\Delta(P, k) = -\psi^S_\Delta(P, k)\tilde{\phi}^1_I \varepsilon^{\beta *}_{\lambda P} w_\beta(P, \lambda_\Delta). \tag{2.5}$$

In this expression, $w_\beta(P, \lambda_\Delta)$ is the Rarita-Schwinger vector spinor [88,89] satisfying the usual auxiliary conditions

$$P^\beta w_\beta = 0, \qquad \gamma^\beta w_\beta = 0, \tag{2.6}$$

and the Dirac equation

$$(\not{P} - M)w_\beta(P, \lambda_\Delta) = 0. \tag{2.7}$$

The function $\tilde{\phi}^1_I = (T \cdot \xi^{1*})\tilde{\chi}_I$ is the isospin part of the state, with T the isospin transition operator, and $\tilde{\chi}_I$ the isospin-3/2 state of projection I.

For a particle of mass m_H and three-momentum P in the z direction, the fixed-axis basis states used in (2.1) and (2.5) are defined as

$$\varepsilon^\mu_{\pm P} = \mp\frac{1}{\sqrt{2}}(0, 1, \pm i, 0)$$
$$\varepsilon^\mu_{0P} = \frac{1}{m_H}(\mathrm{P}, 0, 0, \sqrt{m_H^2 + \mathrm{P}^2}). \tag{2.8}$$

These are the diquark fixed-axis polarization states discussed in great detail in [5]. Here it is sufficient to note that they satisfy the orthogonality condition $P \cdot \varepsilon_{\lambda P} = 0$, and that

$$\sum_\lambda \varepsilon^\mu_{\lambda P}(\varepsilon^\nu_{\lambda P})^* = -g^{\mu\nu} + \frac{P^\mu P^\nu}{m_H^2}. \tag{2.9}$$

Because of the orthogonality condition, the wave functions (2.1) and (2.5) satisfy the Dirac equation for the mass m_H.

As discussed in [5] the fixed-axis diquark polarization states introduce no angular dependence in the wave function, and therefore are convenient to describe S states, without introducing any extra constraint. We will show subsequently here that they are also convenient to define higher angular momentum states.

Finally, for the scalar wave functions ψ^S_N and ψ^S_Δ in (2.1) and (2.5), which describe the relative quark-diquark radial motion, we use the parametrizations

$$\psi_N^S = \frac{N_0}{m_s(\beta_1 + \chi_N)(\beta_2 + \chi_N)}, \tag{2.10}$$

$$\psi_\Delta^S = \frac{N_S}{m_s(\alpha_1 + \chi_\Delta)(\alpha_2 + \chi_\Delta)^2}, \tag{2.11}$$

where

$$\chi_H = \frac{(P-k)^2 - (m_H - m_s)^2}{m_H m_s} \tag{2.12}$$

for $H = N, \Delta$. This parametrization allows for an interplay between two different momentum scales in the problem, quantified by the β_1 and β_2 parameters for the nucleon, and α_1 and α_2 for the Δ.

The factors N_0 and N_S are normalization constants fixed by the condition

$$\int_k [\psi_H^S(\bar{P}, k)]^2 = 1, \tag{2.13}$$

with $\bar{P} = (m_H, 0, 0, 0)$ and the covariant integral $\int_k$ is defined in Eq. (4.3) below. The normalization condition is consistent with the charge constraint

$$Q_I = 3\sum_\lambda \int_k \bar{\Psi}_H^S(\bar{P}, k) j_1(0) \gamma^0 \Psi_H^S(\bar{P}, k), \tag{2.14}$$

where $j_1(0)$ is the isospin part of the quark charge operator, and Q_I is the charge of the state with isospin projection I for either the nucleon ($H = N$ with isospin $1/2$) or the Δ ($H = \Delta$ with isospin $3/2$). See Refs. [4,68] for more details.

In this paper the Δ, with total angular momentum $3/2$, is composed of two positive parity subsystems (the spin $1/2$ quark and the spin 1 diquark). We will refer to the total spin $\mathcal{S}$ of the state as the ''core'' spin, in order to distinguish if from the total angular momentum of the state (also called the ''spin'' of the particle). If the orbital angular momentum between the quark and diquark is zero, then the core spin of the Δ must be $3/2$. However, a state of positive parity and total angular momentum $3/2$ can also be constructed if the orbital angular momentum of the constituents is a D wave ($L = 2$) and the core spin is either $\mathcal{S} = 1/2$ or $\mathcal{S} = 3/2$. (For the nucleon, in contrast, the $L = 2$ orbital state can couple only to the core spin $\mathcal{S} = 3/2$.) The next subsections will define these two possible Δ D states.

B. The two different spin-core D-wave components of the Δ wave function

1. D-wave operator

Turning to the construction of the momentum-space part of the D-wave components of the wave function of the Δ, we start by noting that, in relativity, inner products of three vectors (and, consequently, magnitudes of angles) are not Poincaré invariant. Hence, the operator $\mathcal{D}^{\alpha\beta}$ that generates a D-wave in the relative momentum variable k, only has the pure D-wave structure in the baryon rest frame. In any other (moving) frame the intrinsic D state will generate components in other partial waves. Therefore, we start by defining that operator in the rest frame of the Δ. To find its form in that frame we exploit the two features that define a D wave: (i) $\mathcal{D}^{\alpha\beta}$ is bilinear in the 3-momentum vector part $\mathbf{k}$ in the Δ rest frame, and (ii) the integral of $\mathcal{D}^{\alpha\beta}$ over all the possible directions of $\mathbf{k}$ has to vanish in the rest frame.

It is convenient to introduce a four vector that reduces to the 3-momentum $\mathbf{k}$ in the Δ rest frame. Defining this vector for an arbitrary hadron

$$\tilde{k}^\alpha = k^\alpha - \frac{P\cdot k}{m_H^2} P^\alpha, \tag{2.15}$$

where, in the hadron rest frame, $\tilde{k} = (0, \mathbf{k})$ and $\tilde{k}^2 = -\mathbf{k}^2$. In terms of this vector, the two defining properties of $\mathcal{D}$ lead immediately to the operator

$$\mathcal{D}^{\alpha\beta}(P, k) = \tilde{k}^\alpha \tilde{k}^\beta - \frac{\tilde{k}^2}{3} \tilde{g}^{\alpha\beta}, \tag{2.16}$$

where

$$\tilde{g}^{\alpha\beta} = g^{\alpha\beta} - \frac{P^\alpha P^\beta}{m_H^2}. \tag{2.17}$$

(In this discussion we suppress the subscript H on both $\mathcal{D}$ and $\tilde{k}$, relying on the reader to infer the correct operator from the context.) Note the constraint conditions

$$P_\alpha \mathcal{D}^{\alpha\beta} = 0 = \mathcal{D}^{\alpha\beta} P_\beta. \tag{2.18}$$

It is convenient to work with the spherical components of $\mathcal{D}$, defined to be

$$D_{\lambda,\lambda'} = \varepsilon_{\lambda P}^{\alpha *} \mathcal{D}_{\alpha\beta}(P, k) \varepsilon_{\lambda' P}^{\beta}. \tag{2.19}$$

Using the definition (2.8) of the fixed-axis polarization states, it is easy to see that D is a Hermitian matrix. In the hadron rest frame the matrix elements of D are related directly to the spherical harmonics $Y_{m_l}^L(\mathbf{k})$ with $L = 2$. A representation convenient for later applications is

$$D_{\lambda,\lambda'} = \frac{\sqrt{8\pi}}{3} \mathbf{k}^2 Y_{m_\ell}^2(\hat{\mathbf{k}}) \langle 1\lambda 2 m_\ell | 1\lambda' \rangle, \tag{2.20}$$

where the vector coupling or Clebsch-Gordon (GC) coefficients are denoted as

$$\langle j_1 \mu_1 j_2 \mu_2 | j_{12} \mu_1 + \mu_2 \rangle = C(j_1 j_2 j_{12}; \mu_1 \mu_2). \tag{2.21}$$

Equation (2.20) shows how the operator D can be interpreted as the projection of the incoming direct product state of orbital angular momentum $L = 2 \otimes$ a spin-1 vector $\varepsilon_\lambda^\alpha$, onto an outgoing vector state $\varepsilon_{\lambda'}^*$

$$\sum_{\lambda\lambda'}\varepsilon^{\alpha}_{\lambda}D_{\lambda,\lambda'}\varepsilon^{*}_{\lambda'}=\frac{\sqrt{8\pi}}{3}\mathbf{k}^2\sum_{\lambda\lambda'}\varepsilon^{*}_{\lambda'}\langle 1\lambda 2m_\ell|1\lambda'\rangle Y^2_{m_\ell}(\hat{\mathbf{k}})\varepsilon^{\alpha}_{\lambda}. \tag{2.22}$$

2. Spin-projection operators

To prepare for that construction of the D-wave components of the wave function, we recall the definitions of the spin-projection operators $\mathcal{P}_{1/2}$ and $\mathcal{P}_{3/2}$ previously used in Ref. [68] (and in other works). These are constructed from the operator (2.17) and the operator

$$\tilde{\gamma}^{\alpha}=\gamma^{\alpha}-\frac{\not{P}P^{\alpha}}{m_H^2}. \tag{2.23}$$

The operator has the property

$$\tilde{\gamma}^{\alpha}\tilde{\gamma}_{\alpha}=3. \tag{2.24}$$

In terms of these operators, the projection operators can be written as

$$(\mathcal{P}_{1/2})^{\alpha\beta}=\frac{1}{3}\tilde{\gamma}^{\alpha}\tilde{\gamma}^{\beta}\qquad(\mathcal{P}_{3/2})^{\alpha\beta}=\tilde{g}^{\alpha\beta}-(\mathcal{P}_{1/2})^{\alpha\beta}. \tag{2.25}$$

For details see Refs. [68,90,91]. We note that $\mathcal{P}_{3/2}$ can be cast into the form usually found in the literature,

$$(\mathcal{P}_{3/2})^{\alpha\beta}=g^{\alpha\beta}-\frac{1}{3}\gamma^{\alpha}\gamma^{\beta}-\frac{1}{3m_H^2}(\not{P}\gamma^{\alpha}P^{\beta}+P^{\alpha}\gamma^{\beta}\not{P}), \tag{2.26}$$

and that these spin projectors satisfy the closure and orthogonality relations

$$\begin{aligned}&(\mathcal{P}_{1/2})^{\alpha\beta}+(\mathcal{P}_{3/2})^{\alpha\beta}=\tilde{g}^{\alpha\beta}\\&(\mathcal{P}_{1/2})^{\alpha\beta}(\mathcal{P}_{3/2})_{\beta\gamma}=0=(\mathcal{P}_{3/2})^{\alpha\beta}(\mathcal{P}_{1/2})_{\beta\gamma}.\end{aligned} \tag{2.27}$$

Denoting the operators (2.25) generically by $\mathcal{P}_S$, one easily sees that

$$P_{\alpha}(\mathcal{P}_S)^{\alpha\beta}=0, \tag{2.28}$$

$$[\not{P},\mathcal{P}_S]=0, \tag{2.29}$$

$$\gamma_{\alpha}\mathcal{P}^{\alpha\beta}_{3/2}=0=\mathcal{P}^{\alpha\beta}_{3/2}\gamma_{\beta}. \tag{2.30}$$

Note also that the state functions previously introduced in Eqs. (2.1) and (2.5) satisfy the expected eigenvector equations

$$(\mathcal{P}_{1/2})_{\alpha}{}^{\beta}U_{\beta}=U_{\alpha}\qquad(\mathcal{P}_{3/2})_{\alpha}{}^{\beta}w_{\beta}=w_{\alpha}. \tag{2.31}$$

3. Construction of the two possible D-state components of the Δ

Using the operator $\mathcal{D}$ and the spin-projection operators $\mathcal{P}_S$ introduced above, we can now construct D-state wave functions for the Δ. Just as the S-state wave function is a matrix element of the Δ initial state with a final state consisting of a quark and a diquark in a relative S state, the D-state wave functions are matrix elements of the Δ initial state with a final state consisting of a quark and diquark in a relative D state. The construction is carried out in two steps. First, a D-wave dependence is introduced by contracting the $\mathcal{D}$ operator with the elementary S-wave Rarita-Schwinger wave function w_α, giving the state

$$\mathcal{W}^{\alpha}_{\lambda_\Delta}(P,k)=\mathcal{D}^{\alpha\beta}(P,k)w_{\beta}(P,\lambda_\Delta). \tag{2.32}$$

The resulting state $\mathcal{W}^{\alpha}$ satisfies the Dirac equation. Next, using $P_{\alpha}\mathcal{D}^{\alpha\beta}=0$ and the completeness relation Eq. (2.27) we conclude that this $\mathcal{W}^{\alpha}$ is actually the sum (only) of two *independent* spin components

$$\begin{aligned}\mathcal{W}^{\alpha}_{\lambda_\Delta}(P,k)&=g^{\alpha}{}_{\beta}\mathcal{W}^{\beta}_{\lambda_\Delta}(P,k)\\&=[(\mathcal{P}_{1/2})^{\alpha}{}_{\beta}+(\mathcal{P}_{3/2})^{\alpha}{}_{\beta}]\mathcal{W}^{\beta}_{\lambda_\Delta}(P,k).\end{aligned} \tag{2.33}$$

This leads to the definition of two independent D-wave Δ wave functions

$$\begin{aligned}\phi_{D2S}(\lambda\lambda_\Delta)&=-3\varepsilon^{\beta *}_{\lambda P}(\mathcal{P}_S)_{\beta\alpha}\mathcal{W}^{\alpha}_{\lambda_\Delta}(P,k)\\&=-3\varepsilon^{\beta *}_{\lambda P}(\mathcal{P}_S)_{\beta\alpha}\mathcal{D}^{\alpha\gamma}(P,k)w_{\gamma}(P,\lambda_\Delta),\end{aligned} \tag{2.34}$$

where the factor of -3 has been added for convenience, $S=1/2$ or $3/2$, and $\varepsilon^{*}_{\lambda}$ describes the state of the outgoing diquark, just as in the S-state wave functions Eqs. (2.1) and (2.5). Equation (2.34) defines the spin part of the two D-state wave functions only; isospin and radial parts will be added below. These wave functions satisfy the Dirac Eq. (2.7).

It is interesting to see how the wave functions (2.34) have the correct spin structure corresponding to the two different $(L,\mathcal{S})$ coupling configurations, $(2,\frac{1}{2})$ and $(2,\frac{3}{2})$, both giving total $J=3/2$. Here we summarize the main points; details are given in Appendix A. The first step is to introduce core spin wave functions (direct products of the spin-1 diquark and a spin-1/2 quark) with $\mathcal{S}=1/2$ or $3/2$. These core wave functions, denoted generically by V_S, are constructed using CG coefficients

$$V^{\alpha}_{S}(P,\lambda_s)=\sum_{\lambda}\left\langle\frac{1}{2}\lambda 1\lambda'|S\lambda_s\right\rangle\varepsilon^{\alpha}_{\lambda' P}u_{\Delta}(P,\lambda), \tag{2.35}$$

where u_Δ was defined in Eq. (2.3) [with $H\to\Delta$]. It is easy to see that the V^{α}_{S} satisfy the Dirac Eq. (2.7), that $P_{\alpha}V^{\alpha}_{S}=0$, and it can be shown that they are eigenstates of the projectors $\mathcal{P}_S$. The fact that $V_{3/2}$ also satisfies the special spin 3/2 constraint $\gamma_{\alpha}V^{\alpha}_{3/2}=0$ is shown in Appendix B.

These wave functions are orthonormal and complete

$$\bar{V}_S^{\alpha}(P,\lambda)V_{S\alpha}(P,\lambda') = \delta_{\lambda\lambda'}$$
$$\sum_{\lambda_s} V_S^{\alpha}(P,\lambda_s)\bar{V}_S^{\beta}(P,\lambda_s) = (\mathcal{P}_S)^{\alpha\beta}\left[\frac{m_\Delta + \not{P}}{2m_\Delta}\right]. \tag{2.36}$$

Using the Dirac equation to introduce the projection operator into Eq. (2.34), and then inserting these expansions, allows us to express the D-state wave functions in the form

$$\begin{aligned}\phi_{D2S}(\lambda) &= -3\varepsilon_{\lambda P}^{\beta *}\sum_{\lambda_s} V_{S\beta}(P,\lambda_s)\\ &\quad\times\{\bar{V}_{S\alpha}(P,\lambda_s)\mathcal{D}^{\alpha\gamma}w_\gamma(P,\lambda_\Delta)\}\\ &= (-1)^{S-(1/2)}\sqrt{4\pi}\mathbf{k}^2\varepsilon_{\lambda P}^{\beta *}\sum_{m_\ell}\left\langle 2m_l; S\lambda_s|\frac{3}{2}\lambda_\Delta\right\rangle\\ &\quad\times Y^2_{m_l}V_{S\beta}(P,\lambda_s).\end{aligned} \tag{2.37}$$

This displays the two states as sums over either an $S = 1/2$ or $3/2$ core wave function V_S times an orbital angular momentum $L = 2$ spherical harmonic function $Y^2_{m_l}$ coupled to a spin $3/2$ Δ state, and is demonstrated in Appendix A. Using (2.37) and the normalization of the V_S states, the normalization of the ϕ_{D2S} are

$$\begin{aligned}\frac{1}{4\pi}\int d\Omega_{\hat{\mathbf{k}}}\sum_\lambda|\phi_{D2S}(\lambda\lambda_\Delta)|^2 &= \mathbf{k}^4\sum_{m_\ell}\left\langle 2m_l; S\lambda_s|\frac{3}{2}\lambda_\Delta\right\rangle\\ &= \mathbf{k}^4.\end{aligned} \tag{2.38}$$

Using the definitions (2.34) and adding the isospin factor and scalar wave function, the complete Δ D-state wave functions are

$$\begin{aligned}\Psi^{D1}_\Delta(P,k) &= \phi_{D1}(\lambda)\tilde{\phi}^1_I\psi^{D1}_\Delta(P,k)\\ \Psi^{D3}_\Delta(P,k) &= \phi_{D3}(\lambda)\tilde{\phi}^1_I\psi^{D3}_\Delta(P,k),\end{aligned} \tag{2.39}$$

where the following simple forms were used for the scalar functions ψ^{D1}_Δ and ψ^{D3}_Δ

$$\psi^{D1}_\Delta(P,k) = N_{D1}\left[\frac{1}{m_s^3(\alpha_3+\chi_\Delta)^4)} - \frac{\lambda_{D1}}{m_s^3(\alpha_4+\chi_\Delta)^4}\right], \tag{2.40}$$

$$\psi^{D3}_\Delta(P,k) = \frac{N_{D3}}{m_s^3(\alpha_5+\chi_\Delta)^4}. \tag{2.41}$$

The D1 state has two range parameters (α_3 and α_4) and the D3 state only one (α_5). The three parameters are adjusted to the data. We anticipate that our numerical results for the range parameters are consistent with an expected longer range (in r space) for the D states relative to the S state. Note that the definition of $\mathcal{D}$ guarantees also that the D-state wave function will go as $\mathbf{k}^2$ when $\mathbf{k}\to 0$, as expected [92], and an additional mass factor m_s^{-2} is introduced to compensate for the dimensions introduced by this $\mathbf{k}^2$ dependence of the $\mathcal{D}$ matrix (so that the product of $\mathcal{D}$ with ψ^{D1}_Δ or ψ^{D3}_Δ have no dimensions). The power 4 in the denominators of the previous equations was chosen to reproduce the expected pQCD behavior for large Q^2 ($G_E^* \sim 1/Q^4$, $G_C^* \sim 1/Q^6$) [16], and also to assure the convergence of the normalization integrals

Combining Eqs. (2.5) and (2.39), the total Δ wave function can be written as

$$\Psi_\Delta = N[\Psi^S_\Delta + a\Psi^{D3}_\Delta + b\Psi^{D1}_\Delta], \tag{2.42}$$

where a and b are admixture coefficients. The D1 component with core spin $1/2$ is orthogonal to both of the other components because of the orthogonality condition (2.27), and the two components with core spin $3/2$, Ψ^{D3}_Δ and Ψ^S_Δ, are orthogonal because the overlap integral is linear in $\int_k Y_{20}(z) = 0$. We will chose to normalize the individual states to unity, giving $N = 1/\sqrt{1+a^2+b^2}$ for the overall normalization factor.

C. Normalization and orthogonality condition

The individual D-wave scalar wave function will be chosen to satisfy the normalization conditions

$$\int_k\{\tilde{k}^4[\psi^{D2S}_\Delta(\bar{P},k)]^2\} = 1. \tag{2.43}$$

This determines the coefficients N_{D1} (as a function of λ_{D1}) and N_{D3}.

The two components Ψ^S_Δ and Ψ^{D3}_Δ are orthogonal to the nucleon S-state Ψ^S_N, but the component Ψ^{D1}_Δ is, in general, not orthogonal to the nucleon S state. This happens because both wave functions have a core spin $S = 1/2$, and even though the D1 state depends on $Y^2_{m_\ell}$, it is impossible for both particles to sit simultaneously in their rest frame, so the angular integral always has some other angular dependence that prevents it from being exactly zero. The orthogonality condition

$$\sum_\lambda\int_k\bar{\Psi}^{D1}_\Delta(\bar{P}_+,k)\Psi^S_N(\bar{P}_-,k) = 0, \tag{2.44}$$

where $\bar{P}_+$, $\bar{P}_-$ represent the baryon momenta for $Q^2 = 0$, must be imposed numerically, and this can be done only at one value of Q^2. This condition determines λ_{D1}. As we will see below, our treatment of gauge invariance requires that we impose the condition (2.44) at the point $Q^2 = 0$. Working in the Δ rest frame, the momenta $\bar{P}_+$ and $\bar{P}_-$ are therefore

$$\begin{aligned}\bar{P}_+ &= (M,0,0,0)\\ \bar{P}_- &= \left(\frac{M^2+m^2}{2M},0,0,-\frac{M^2-m^2}{2M}\right).\end{aligned} \tag{2.45}$$

To determine the coefficients N_{D1} and λ_{D1} in the D1 component, we first fix α_3 and α_4. Then λ_{D1} is determined by (2.44), and finally the value of N_{D1} fixed by the normalization condition (2.43).

D. Properties of the wave functions under a Lorentz transformation

The form for the wave functions given in Eq. (2.39) holds only for the case where the particle is moving along the z direction [with 4-momentum $P = (\sqrt{m_H^2 + \mathrm{P}^2}, 0, 0, \mathrm{P})$]. The generic wave function can be obtained from an arbitrary Lorentz transformation Λ

$$P'^{\mu} = \Lambda^{\mu}_{\nu} P^{\nu}. \tag{2.46}$$

Under a Lorentz transformation we obtain

$$\begin{aligned} &\varepsilon^{\mu}_{P'} = \Lambda^{\mu}_{\nu}\varepsilon^{\nu}_{P} \qquad w'_{\beta}(P') = \Lambda_{\beta}{}^{\alpha} S(\Lambda) w_{\alpha}(P) \\ &u'(P') = S(\Lambda)u(P) \qquad \mathcal{D}_{\alpha\beta}(P', k') = \Lambda_{\alpha}{}^{\sigma}\Lambda_{\beta}{}^{\rho}\mathcal{D}_{\sigma\rho}(P, k) \\ &S^{-1}(\Lambda)(\mathcal{P}'_S)_{\alpha\beta}S(\Lambda) = \Lambda_{\alpha}{}^{\sigma}\Lambda_{\beta}{}^{\rho}(\mathcal{P}_S)_{\sigma\rho}, \end{aligned} \tag{2.47}$$

where u' and w'_{β} represent the states in the arbitrary frame. For simplicity, the dependence of the spinor states on the Wigner rotations acting on the polarization vectors has not been shown explicitly, and $(\mathcal{P}_S)$ are the projectors of (2.25) with $(\mathcal{P}'_S)$ the same projectors with $P' = \Lambda P$, one obtains the transformation law

$$\mathcal{Z}'_{\beta}(P', k') = S(\Lambda)\Lambda_{\beta}{}^{\alpha}\mathcal{Z}_{\alpha}(P, k) \tag{2.48}$$

for any vector-spinor state $\mathcal{Z}$. Finally, from (2.48) the transformation laws for the total Δ wave function follows

$$\Psi'_{\Delta}(P', k') = S(\Lambda)\Psi_{\Delta}(P, k). \tag{2.49}$$

In conclusion, we may derive the baryon wave function in any frame, where the four-momentum P is arbitrary, by means of a Lorentz transformation Λ on the wave function defined in the baryon rest frame.

III. FORM FACTORS FOR THE $\gamma N \to \Delta$ TRANSITION

A. Definitions

The electromagnetic $N\Delta$ transition current is

$$J^{\mu} = \bar{w}_{\beta}(P_+)\Gamma^{\beta\mu}(P, q)\gamma_5 u(P_-)\delta_{I'I}, \tag{3.1}$$

where P_+ (P_-) is the momentum of the Δ (nucleon), I' (I) the isospin projection of the Δ (nucleon), and the operator $\Gamma^{\beta\nu}$ can be written in general [93] as

$$\Gamma^{\beta\mu}(P, q) = G_1 q^{\beta}\gamma^{\mu} + G_2 q^{\beta}P^{\mu} + G_3 q^{\beta}q^{\mu} - G_4 g^{\beta\mu}. \tag{3.2}$$

Although we have omitted the helicity indices for these states, the transition current depends on both the helicities of the final and initial baryons and on the photon helicity. The variables P and q are, respectively, the average of baryon momenta and the absorbed (photon) momentum

$$P = \frac{1}{2}(P_+ + P_-) \qquad q = P_+ - P_-. \tag{3.3}$$

The form factors G_i, $i = 1, \ldots, 4$ are functions of $Q^2 = -q^2$ exclusively. Because of current conservation, $q_{\mu}\Gamma^{\beta\mu} = 0$, only three of the four form factors are independent. In particular, we can write G_4 in terms of the other three form factors as

$$G_4 = (M + m)G_1 + \frac{M^2 - m^2}{2}G_2 - Q^2 G_3, \tag{3.4}$$

and adopt the structure originally proposed by Jones and Scadron [93]. Alternatively (see below), we can write G_3 in terms of the other three

$$G_3 = \frac{1}{Q^2}\left[(M + m)G_1 + \frac{M^2 - m^2}{2}G_2 - G_4\right]. \tag{3.5}$$

The parametrization (3.2) in terms of the form factors G_i is not the most convenient one for comparison with the experimental data. More convenient are the magnetic dipole (M), electric quadrupole (E), and Coulomb quadrupole (C) form factors. These can be defined directly in terms of helicity amplitudes [16,93]. *Note that the form factor G_3 does not enter directly into the expressions for the helicity amplitudes* because $\epsilon^{\mu *}_{\lambda} q_{\mu} = 0$ for all λ. But, if we use the constraint (3.4) to eliminate G_4, G_3 appears in these expressions and we obtain

$$\begin{aligned} G^*_M(Q^2) = \kappa\Big\{&[(3M + m)(M + m) + Q^2]\frac{G_1}{M} \\ &+ (M^2 - m^2)G_2 - 2Q^2 G_3\Big\}, \end{aligned} \tag{3.6}$$

$$\begin{aligned} G^*_E(Q^2) = \kappa\Big\{&(M^2 - m^2 - Q^2)\frac{G_1}{M} + (M^2 - m^2)G_2 \\ &- 2Q^2 G_3\Big\}, \end{aligned} \tag{3.7}$$

$$\begin{aligned} G^*_C(Q^2) = \kappa\{&4MG_1 + (3M^2 + m^2 + Q^2)G_2 \\ &+ 2(M^2 - m^2 - Q^2)G_3\}, \end{aligned} \tag{3.8}$$

where

$$\kappa = \frac{m}{3(M + m)}. \tag{3.9}$$

These three form factors G^*_a ($a = M, E, C$) are, respectively, the magnetic, electric and Coulomb (or scalar) multipole transition form factors.

As G^*_M dominates at low momentum Q^2, the following ratios are useful

$$R_{EM}(Q^2) = -\frac{G^*_E(Q^2)}{G^*_M(Q^2)}, \tag{3.10}$$

and

$$R_{SM}(Q^2) = -\frac{|\mathbf{q}|}{2M}\frac{G^*_C(Q^2)}{G^*_M(Q^2)}, \tag{3.11}$$

where $\mathbf{q}$ is the photon 3-momentum in the Δ rest frame

$$|\mathbf{q}| = \frac{\sqrt{d_+ d_-}}{2M}, \tag{3.12}$$

with

$$d_\pm = (M \pm m)^2 + Q^2. \tag{3.13}$$

The analysis of the transition at large Q^2 in the pQCD regime (where quarks and gluons are the appropriate degrees of freedom) gives $G_M^* \simeq -G_E^* \sim 1/Q^4$ and $G_C^* \sim 1/Q^6$ [16].

B. The G_1, G_2, G_3 set versus the G_1, G_2, G_4 set

The representation of the electromagnetic current in terms of the 3 independent (G_1, G_2, G_3) form factors, as proposed by Jones and Scadron [93], is not the most convenient choice that can be made. As mentioned above, the form factor G_3 is not part of the helicity transition amplitudes given by the operator $\varepsilon_\mu(q)J^\mu$, due to the condition $\varepsilon \cdot q = 0$. For this reason it seems natural to replace the set (G_1, G_2, G_3) by (G_1, G_2, G_4). On this basis, G_M^*, G_E^*, and G_C^* are given by

$$G_M^* = \kappa\left\{2G_4 + d_+ \frac{G_1}{M}\right\}, \tag{3.14}$$

$$G_E^* = \kappa\left\{2G_4 - d_+ \frac{G_1}{M}\right\}, \tag{3.15}$$

$$G_C^* = \frac{\kappa}{Q^2}\{2(M-m)d_+ G_1 + d_+ d_- G_2 - 2(M^2 - m^2 - Q^2)G_4\}, \tag{3.16}$$

where $d_\pm$ were defined in Eq. (3.13). Note that the multipole form factors G_M^* and G_E^* do not depend on G_2.

Equation (3.16) for G_C^* presents an apparent singularity when $Q^2 = 0$. The presence of this apparent singularity is the historical reason for choosing G_1, G_2, G_3 to be the independent form factors; this choice gives finite form factors under any circumstances. However, if the theory conserves current, *with a G_3 that is finite at $Q^2 = 0$* (a required feature of any consistent model), then the singularity disappears as $Q^2 \to 0$, since, using the current conservation condition (3.5), the numerator (at $Q^2 = 0$) is proportional to

$$\left[(M+m)G_1 + \frac{M^2 - m^2}{2}G_2 - G_4\right] = Q^2 G_3, \tag{3.17}$$

which, if G_3 is finite, approaches zero as $Q^2 \to 0$.

We prefer the independent choice G_1, G_2, G_4 because it enables us to discuss the restrictions imposed by current conservation in a more transparent way. Many models do not automatically conserve current (this is true for our D1 component, as we will discuss below). If we start with a model that does not naturally conserve current, we prefer to impose current conservation by modifying the current in the following way:

$$J^\mu \to J^\mu + \frac{(q \cdot J)}{Q^2} q^\mu. \tag{3.18}$$

This way of imposing current conservation is, of course, not unique, but has the nice property that the additional term added is proportional to q^μ, and hence makes *no additional contributions to any observables obtained by contracting the current with another conserved current or with a photon polarization vector*, always orthogonal to q^μ (in the Lorentz gauge, our choice). In the application discussed in this paper, the modification (3.18) will only alter the G_3 form factor, and when we use the expressions (3.14), (3.15), and (3.16) we see that they are unchanged by any modification of G_3. Hence, our method allows us to choose G_3 to satisfy current conservation, without changing the basic predictions of the theory.

However, current conservation is like the Cheshire cat, while the consequences of imposing it seem to have vanished, a "smile" still remains. What remains is the requirement that there is no singularity in G_C^* as $Q^2 \to 0$. This requirement is satisfied by modifying the form factors in such a way that the linear combination (3.17) is zero at $Q^2 = 0$. Implementation of this requirement will be discussed below.

C. Simple relation for G_C^*

In the following discussion we will work in the rest frame of the outgoing Δ, where the four-momenta (3.3) become

$$q^\mu = (\omega, 0, 0, |\mathbf{q}|) \qquad P^\mu = \left(\frac{2M - \omega}{2}, 0, 0, -\frac{|\mathbf{q}|}{2}\right), \tag{3.19}$$

where $|\mathbf{q}|$ was given in Eq. (3.12), and the photon energy ω can be written in terms of the nucleon energy $\omega = M - \sqrt{m^2 + |\mathbf{q}|^2}$, or

$$\omega = \frac{P_+ \cdot q}{M} = \frac{M^2 - m^2 - Q^2}{2M}. \tag{3.20}$$

In this frame the photon moves in the $+\hat{z}$ direction, with polarization vectors

$$\epsilon^\mu_{\pm q} = \mp\frac{1}{\sqrt{2}}(0, 1, \pm i, 0) \qquad \epsilon^\mu_{0q} = \frac{1}{Q}(|\mathbf{q}|, 0, 0, \omega). \tag{3.21}$$

Note that the transverse states ($\lambda = \pm 1$) are identical to those defined in Eq. (2.8), but that the longitudinal state is very different. All of these satisfy the constraint $q_\mu \epsilon^\mu_\lambda = 0$, and because $q^z > 0$ are identical to helicity states. While we will work out the explicit relations in this rest frame, all relations that are derived from four-vector scalar products are, of course, independent of the frame.

Introduce the photon helicity amplitudes of the electromagnetic transition current (3.1) (for a general discussion of helicity amplitudes see Refs. [16,93])

$$\epsilon^{\mu}_{\lambda q} J_{\mu} = \mathcal{J}_{\lambda}, \tag{3.22}$$

where the polarizations of the N and Δ will remain unspecified. Note immediately that G_3 does not contribute to any of these amplitudes, and because $P \cdot \epsilon_{\pm} = 0$, the transverse amplitudes do not depend on G_2. The only amplitude that depends on G_2 is the longitudinal $\mathcal{J}_0$. Using the relations

$$\epsilon^{\mu}_{0q} P_{\mu} = \frac{|\mathbf{q}|M}{Q} \equiv \frac{1}{a_P} \qquad \epsilon^{\mu}_{0q} = a_q q^{\mu} + a_P P^{\mu}; \qquad a_q = \frac{M^2 - m^2}{2|\mathbf{q}|QM}, \tag{3.23}$$

we can reduce the terms $\not{\epsilon}_{0q}$ and ϵ^{β}_{0q} that occur when using (3.1) to evaluate $\mathcal{J}_0$, and obtain

$$\mathcal{J}_{0\,s's} = \mathcal{R}_{s's} \frac{(M+m)}{2m} \frac{3Q}{\sqrt{d_+ d_-}} G_C^*, \tag{3.24}$$

where s and s' are, respectively, the nucleon and Δ spin projections along the z-axis, and

$$\mathcal{R}_{s's} = \bar{w}_{\beta}(P_+, s') q^{\beta} \gamma_5 u(P_-, s) = \delta_{ss'}(2s) \sqrt{\frac{2d_+}{3mM}} \frac{d_-}{4M}. \tag{3.25}$$

We emphasize that, provided we use Eq. (3.16) to define G_C^*, this relation holds for all models, *even those that do not conserve current*. Note that $\mathcal{R} \neq 0$ only if the spin projections are equal ($s = s'$). We may conclude that $G_C^* \neq 0$ only if (for example) $\mathcal{J}_{0\,(1/2)(1/2)} \neq 0$, and using Eq. (3.24) we obtain

$$\mathcal{J}_{0\,(1/2)(1/2)} = \frac{(M+m)}{4m} \sqrt{\frac{3d_-}{2mM}} \left[\frac{Q}{M}\right] G_C^*. \tag{3.26}$$

IV. THE ELECTROMAGNETIC CURRENT WITHIN THE SPECTATOR MODEL

In this section we study how the electromagnetic current can be constructed within the constituent quark model (CQM) for the baryon structure presented in Sec. II.

In any CQM model the quarks making up the baryons are not point particles, but composite valence quarks, dressed by their gluon and sea quark structure. Here we use the covariant spectator theory and assume the baryon is a quark-diquark system, as explained in Sec. II.

The on-shell diquark mass m_s scales out from the elastic form factor, which turns out to be independent of the diquark mass [4]. This mass does not scale out of the deep inelastic results and the qualitative description of deep inelastic results leads to the estimate of $m_s \simeq 0.8m$, allowing a natural interplay between low and high energy phenomenology. This interplay is needed since the factorization into low and high energy scales does not apply exactly.

In the following, we will explain how gauge invariance conveniently constrains the current, when the internal structure of the quarks is parametrized in terms of phenomenologically fixed wave functions.

A. Implications of the choice of current

1. Simple current

Constituent quarks are dressed particles with a complex effective structure, an effective charge, and magnetic moment. Therefore, their current consists of a Dirac and a Pauli term, and can be written as

$$j^{\mu}_{Ia} = j_1 \gamma^{\mu} + j_2 \frac{i\sigma^{\mu\nu} q_{\nu}}{2m}. \tag{4.1}$$

(The subscript "a" on the current will be dropped in subsequent discussion, and will be used only when we need to distinguish this current from the modified current discussed in the next subsection.) The form factors j_1 and j_2 are normalized in order to describe the nucleon charge and magnetic moments (as functions of the quark isospin I) as discussed in Ref. [4]. The explicit formulas are defined by the Eqs. (4.15) and (7.1) below. The quark current (4.1) is not of the most general form. In the next subsection we will consider a more generic case, in light of the discussion on gauge invariance that unfolds immediately here as consequence of (4.1).

To start this discussion, given the quark current (4.1) and the nucleon (Ψ_N) and Δ (Ψ_{Δ}) wave functions, we write the transition current between these states. With a positive parity axial diquark the only allowed states for the nucleon and Δ are S and D states, since P states are ruled out (unless they are associated with the lower relativistic components, not discussed so far in this series of papers).

To simplify the formulas we will exclude the isospin from the discussion (later in this paper we show how to include the isospin explicitly). In impulse approximation [4,68,94–97] the transition current takes the form

$$J^{\mu} = 3 \sum_{\lambda} \int_k \bar{\Psi}_{\Delta} j^{\mu}_I \Psi_N, \tag{4.2}$$

where all momenta and spin projections (s' for the Δ and s for the nucleon) have been suppressed. The factor 3 sums up the contributions of the three quarks, the sum is over all intermediate polarizations λ of the diquark, and

$$\int_k \equiv \int \frac{d^3k}{(2\pi)^3 2E_s} \tag{4.3}$$

is the covariant integral with $E_s = \sqrt{m_s^2 + \mathbf{k}^2}$ as the diquark on-mass-shell energy. The initial and final momentum dependence are not explicitly included for simplicity.

As discussed in ,Eq. (4.2), for the states Ψ_Δ and Ψ_N defined here, goes beyond the scope of the relativistic impulse approximation shown diagrammatically in Fig. 2, and includes some effective two-body currents.

Since both the final and initial states satisfy the Dirac equation $\not{P}_+\Psi_\Delta = M\Psi_\Delta$ and $\not{P}_-\Psi_N = m\Psi_N$, the Pauli current can be simplified using the Gordon decomposition

$$\sum_\lambda \int_k \bar{\Psi}_\Delta \frac{i\sigma^{\mu\nu}q_\nu}{2m}\Psi_N = \frac{M+m}{2m}\sum_\lambda \int_k \bar{\Psi}_\Delta \gamma^\mu \Psi_N - \frac{(P_+ + P_-)^\mu}{2m}\sum_\lambda \int_k \bar{\Psi}_\Delta \Psi_N. \tag{4.4}$$

The last term is proportional to (inserting the spin projections for clarity)

$$\rho_{s's}(Q^2) \equiv \sum_\lambda \int_k \bar{\Psi}_{\Delta s'}\Psi_{Ns}. \tag{4.5}$$

With this definition (dropping references to s' and s again), we can use the Gordon decomposition to write the current (4.2) as

$$J^\mu = 3j_v \sum_\lambda \int_k \bar{\Psi}_\Delta \gamma^\mu \Psi_N - 3j_2 \frac{P^\mu}{m}\rho(Q^2), \tag{4.6}$$

where

$$j_v = j_1 + \frac{M+m}{2m}j_2. \tag{4.7}$$

These equations hold in any frame.

Next, using Eq. (4.6), the relations (3.23), and the Dirac equation, we find an alternative form for the longitudinal current

$$\mathcal{J}_0 = 3j_v \sum_\lambda \int_k \bar{\Psi}_\Delta \not{\epsilon}_{0q}\Psi_N - 3j_2 \frac{|\mathbf{q}|M}{Qm}\rho(Q^2) = \frac{3}{Q}\sqrt{\frac{d_-}{d_+}}(M+m)j_C\rho(Q^2), \tag{4.8}$$

where

$$j_C = j_1 - j_2\frac{Q^2}{2m(M+m)}. \tag{4.9}$$

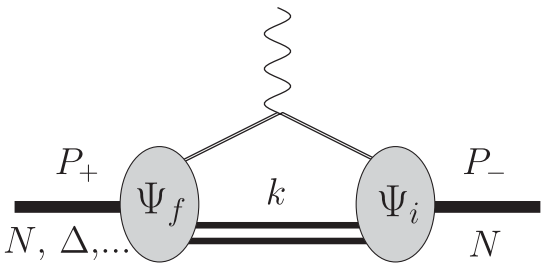

FIG. 2. Relativistic impulse approximation.

Both the current $\mathcal{J}_0$ and the factor ρ depend on the spin projections s' and s, suppressed so far. Taking the spin projections $s = s' = \frac{1}{2}$ and combining this result with Eq. (3.26) gives G_C^* in terms of $\rho_{(1/2)(1/2)}$

$$G_C^*(Q^2) = \frac{4mM}{Q^2}\sqrt{\frac{6Mm}{d_+}}j_C\rho_{(1/2)(1/2)}(Q^2). \tag{4.10}$$

This result holds in any frame.

Now, we connect some of these results to the divergence of the simple current (4.1). Noting that the Pauli term, proportional to j_2, is automatically conserved, the divergence of current depends only on the behavior of the Dirac term, proportional to j_1. Evaluating the divergence gives

$$q\cdot J = 3j_1\sum_\lambda \int_k \bar{\Psi}_\Delta \not{q}\Psi_N = 3(M-m)j_1\rho(Q^2). \tag{4.11}$$

Because the masses are different ($M \neq m$) this (frame independent) result shows that the *simple current* (4.1) will be conserved for an electromagnetic transition from a state Ψ_N to a state Ψ_Δ if and only if $\rho(Q^2) = 0$. We showed in Ref. [68] that this term will vanish identically (for all values of Q^2) if the core spins of the two states are different. This is true for the nucleon S state to Δ S-state transition, and also for the transition from the nucleon S state to the Δ D3 state. It is not true for the transition to the D1 state, as discussed briefly above, and in more detail below.

Combining Eqs. (4.10) and (4.11) gives the following interesting connection

$$q\cdot J_{(1/2)(1/2)} = 3(M-m)\frac{j_1}{j_C}\sqrt{\frac{d_+}{6mM}}\frac{Q^2}{4mM}G_C^*. \tag{4.12}$$

The consequence of this equation is that the simple current (4.1) will be conserved if and only if $G_C^* = 0$. Alternatively, since transitions to the Δ S and D3 states conserve the current (4.1), these *cannot* give a nonzero G_C^*. To build a model in which $G_C^* \neq 0$ we must find a different current, and this leads us to the next subsection.

2. Modified current

Following a previous work [4] we replace the quark current (4.1) by

$$j_I^\mu = j_1\left(\gamma^\mu - \frac{\not{q}q^\mu}{q^2}\right) + j_2\frac{i\sigma^{\mu\nu}q_\nu}{2m} = j_{Ia}^\mu + \Delta j_I^\mu. \tag{4.13}$$

It is easy to evaluate the additional term

$$\Delta j_I^\mu = 3(M-m)\frac{q^\mu}{Q^2}\rho(Q^2). \tag{4.14}$$

This shows that all the *good* properties of the previous current remain intact; when $\rho = 0$ for all Q^2 values, the Dirac current $j_1\gamma^\mu$ is conserved and the correction term vanishes identically. The advantage of the current (4.13) is

that current conservation is guaranteed, even when $\rho(Q^2)$ does not vanish identically.

The only possible problem with the new current is that it might be singular at $Q^2 = 0$. This singularity must be removed by imposing the requirement that $\rho(Q^2) \to Q^2$ as $Q^2 \to 0$. Since $\epsilon_{0q} \cdot q = 0$, Eqs. (4.8) and (4.10) are unchanged, and this requirement also means that G_C^* is finite at $Q^2 = 0$, guaranteeing that the apparent singularity in Eq. (3.16) does indeed cancel.

The condition that guarantees that $\rho = 0$ at $Q^2 = 0$ was already introduced above in Sec. II C, Eq. (2.44). The importance of this orthogonality condition was emphasized in Ref. [98]; imposing it ensures that the current (4.13) is well defined and conserved for all Q^2.

To summarize, in the present model the orbital angular momentum states are not derived from an underlying Hamiltonian. Therefore, the Δ state with $(L, \mathcal{S}) = (2, \frac{1}{2})$, with the same core spin quantum numbers as the nucleon state, even though carrying the correct spin-isospin symmetries, does not have a spacial scalar part ψ_Δ^{D1} that is *ab initio* orthogonal to a nucleon state. The orthogonality is imposed by a judicious choice of the parameter λ_{D1} in Eq. (2.40).

B. Isospin dependence of the current

For simplicity, we did not include isospin in the discussion in the previous subsection. It is included in the definition of the current subsection through the following isoscalar and isovector decomposition, as in Ref. [4]:

$$j_i = \frac{1}{6} f_{i+}(Q^2) + \frac{1}{2} f_{i-}(Q^2)\tau_3, \tag{4.15}$$

where $i = 1$, 2 and $f_{1\pm}$ and $f_{2\pm}$ were adjusted by the charge and magnetic form factors of the nucleon and were normalized to $f_{1\pm}(0) = 1$, $f_{2\pm}(0) = \kappa_\pm$. Only the isovector form factors, f_{i-} contribute to the $\gamma N \to \Delta$ transitions.

The overall isospin factor can be calculated separately, and was worked out in Ref. [68]. This factor is

$$C_{I'I} \equiv \tilde{\phi}^1_{I'} \frac{\tau_3}{2} \phi^1_I = -\frac{1}{\sqrt{3}} \sum_i \chi^\dagger_{\Delta I'} T^i \frac{\tau_3}{2} \tau^i \chi_{NI}$$
$$= -\frac{\sqrt{2}}{3} \delta_{I'I} = C_0 \delta_{I'I}. \tag{4.16}$$

All formulas derived in the previous sections are still valid if we replace

$$j_i \to C_0 f_{i-}. \tag{4.17}$$

V. VALENCE QUARK CONTRIBUTION FOR THE FORM FACTORS

The impulse approximation for $\gamma N \to \Delta$ transitions from the nucleon S state to each of the Δ states can be written, using Eq. (2.42)

$$J^\mu = N[J^\mu_S + a J^\mu_{D3} + b J^\mu_{D1}], \tag{5.1}$$

where the index identifies the Δ state. From this we can calculate the form factors G_1, G_2, and G_4 defined in Eqs. (3.1) and (3.2), and using the definitions given in Eqs. (3.14), (3.15), and (3.16) calculate the multipole transition form factors G_M^*, G_E^* and G_C^*.

A. Transition to the Δ S state

The transition current from the nucleon S state for the Δ S state was already evaluated in Ref. [68]. Using the upper index S to indicate the Δ state, the results are

$$G_M^S(Q^2) = \frac{8}{3\sqrt{3}} \frac{m}{M+m} f_v \mathcal{I}_S, \tag{5.2}$$

$$G_E^S(Q^2) = 0 \qquad G_C^S(Q^2) = 0, \tag{5.3}$$

where j_v is the analogue of (4.7)

$$f_v = f_{1-} + \frac{M+m}{2m} f_{2-}, \tag{5.4}$$

and

$$\mathcal{I}_S = \int_k \psi^S_\Delta(P_+, k) \psi^S_N(P_-, k) \tag{5.5}$$

is the overlap integral of the radial (scalar) wave functions. Asymptotically, we have $G_M^S \sim 1/Q^4$, as showed in Ref. [68].

According to Eqs. (3.15) and (3.16), G_E^S and G_C^S vanish because the terms involving G_1, G_2, and G_4. cancel exactly.

B. Transitions to the Δ D states

The transition currents to the D states are

$$J^\mu_{D2S} = 3 \sum_\lambda \int_k \bar{\Psi}^{D2S}_\Delta(P_+, k) j^\mu_I \Psi_N(P_-, k)$$
$$= \bar{w}_\beta(P_+) \Gamma^{\beta\mu}_{D2S}(P, q) \gamma_5 u_N(P_-) \delta_{I''I}, \tag{5.6}$$

where we suppress all reference to the spins of the nucleon and Δ. Substituting for Ψ_N using Eq. (2.1), Ψ^{D2S}_Δ using Eqs. (2.34) and (2.39), and using the general reduction (4.6) gives

$$\Gamma^{\beta\mu}_{D2S}(P, q) = -3\sqrt{\frac{3}{2}} C_0 \int_k \Big\{ \mathcal{D}^{\beta\beta'}(P_+, k) (\mathcal{P}_\mathcal{S})_{\beta'\alpha'} \sum_{i=1}^{2} \mathcal{O}^\mu_i$$
$$\times \Delta^{\alpha'\alpha} \Big(\gamma_\alpha + \frac{(P_-)_\alpha}{m} \Big) \Big\} \psi^{D2S}_\Delta \psi^S_N, \tag{5.7}$$

where $\Delta^{\beta\alpha}$ is the sum over the fixed-axis diquark polarizations (previously derived in Refs. [5,68])

$$\Delta^{\alpha'\alpha} = \sum_\lambda \varepsilon^{\alpha'}_{\lambda P_+}\varepsilon^{\alpha *}_{\lambda P_-} = -\left(g^{\alpha'\alpha} - \frac{P_-^{\alpha'}P_+^{\alpha}}{b}\right) + a\left[P_-^{\alpha'} - \frac{b}{M^2}P_+^{\alpha'}\right] \times \left[P_+^{\alpha} - \frac{b}{m^2}P_-^{\alpha}\right], \tag{5.8}$$

with

$$a = -\frac{Mm}{b(Mm+b)} \qquad b = P_+\cdot P_-, \tag{5.9}$$

and the two current operators emerging from the reduction (4.6) are

$$\mathcal{O}_1^{\ \mu} = f_v\gamma^\mu \qquad \mathcal{O}_2^{\mu} = -f_{2-}\frac{P^\mu}{m}. \tag{5.10}$$

Using the conditions (2.4), (2.6), and (2.28), the part of the expression for Γ_{D2S} in curly brackets {} reduces to

$$\Gamma^{\beta\mu}_{D2S}(P,q) = -\sqrt{3}\int_k\left\{\mathcal{D}^{\beta\beta'}(P_+,k)(\mathcal{P}_S)_{\beta'\alpha}\sum_{i=1}^{2}\mathcal{O}_i^{\mu} \times\left(\gamma^\alpha - \frac{P_-^\alpha[\not{P}_+ - M]}{mM+b}\right)\right\}\psi_\Delta^{D2S}\psi_N^S. \tag{5.11}$$

This general expression may be reduced further by noting that, in a collinear frame in which none of the momenta have components in the $\hat{x}$ or $\hat{y}$ directions, the only dependence of the integrand on the azimuthal angle φ is in the angular dependent term $\mathcal{D}$. Hence, we may average over this angle using the (covariant) identity

$$\frac{1}{2\pi}\int d\varphi\mathcal{D}^{\alpha\beta}(P_+,k) = b(\tilde{k},\tilde{q})R^{\alpha\beta}(P_+,P_-), \tag{5.12}$$

where

$$b(\tilde{k},\tilde{q}) = \frac{3}{2}\frac{(\tilde{k}\cdot\tilde{q})^2}{\tilde{q}^2} - \frac{1}{2}\tilde{k}^2 \qquad R^{\alpha\beta}(P_+,P_-) = \frac{\tilde{q}^\alpha\tilde{q}^\beta}{\tilde{q}^2} - \frac{1}{3}\tilde{g}^{\alpha\beta}, \tag{5.13}$$

with $\tilde{k}$ and $\tilde{q}$ defined as in Eq. (2.15) [with the substitutions $P\to P_+$ and $m_H\to M$]. This identity is proved in Appendix B.

Using the conditions (2.6) and (2.28) again, the φ average of (5.11) can be simplified

$$\bar{\Gamma}^{\beta\mu}_{D2S}(P,q) = -\sqrt{3}\int_k\left\{b(\tilde{k},\tilde{q})\left[\frac{q^\beta q^{\beta'}}{\tilde{q}^2}(\mathcal{P}_S)_{\beta'\alpha} - \frac{1}{3}\delta_{2S,3}g_\alpha^\beta\right]\times\sum_{i=1}^{2}\mathcal{O}_i^{\mu}\left(\gamma^\alpha - \frac{P_-^\alpha[\not{P}_+ - M]}{mM+b}\right)\right\} \times\psi_\Delta^{D2S}\psi_N^S. \tag{5.14}$$

This will now be evaluated for the two cases of interest.

1. Nucleon $(S)\to\Delta(D3)$

The term in round brackets in Eq. (5.11) commutes with $\mathcal{O}_2$ (an identity operator on the Dirac space), and hence, for the transition to the spin 3/2 core state (D3) with $\mathcal{P}_S = \mathcal{P}_{3/2}$ gives zero (this is the ρ term discussed above). Commuting the term in round brackets through $\mathcal{O}_1$, letting $\not{P}_+\to M$ when it operates to the left, gives

$$\gamma^\mu\left(\gamma^\alpha - \frac{P_-^\alpha[\not{P}_+ - M]}{mM+b}\right) = 2g^{\alpha\mu} - \gamma^\alpha\gamma^\mu - \left(\frac{P_-^\alpha[2P_+^\mu - 2M\gamma^\mu]}{mM+b}\right). \tag{5.15}$$

For the $S=3/2$ case under consideration, the $\gamma^\alpha\gamma^\mu$ terms vanishes, and combining this with the remaining terms gives

$$\bar{\Gamma}^{\beta\mu}_{D3}(P,q) = -2\sqrt{3}f_v\int_k\left\{b(\tilde{k},\tilde{q})\left[\frac{q^\beta q^{\beta'}}{\tilde{q}^2}(\mathcal{P}_{3/2})_{\beta'\alpha} - \frac{1}{3}g_\alpha^\beta\right]\times\left(g^{\alpha\mu} - \frac{P_-^\alpha[P_+^\mu - M\gamma^\mu]}{mM+b}\right)\right\} \times\psi_\Delta^{D3}\psi_N^S. \tag{5.16}$$

Now, we know that the terms proportional to q^μ can be ignored (they determine G_3, which we already know is just right to give a gauge invariant result, but otherwise play no role in the calculation). Furthermore, we already know that $G_C^* = 0$, and hence the value of G_2 must be fixed in terms of G_1 and G_4 through Eq. (3.16), so we need not calculate it explicitly. This leaves only G_1 and G_4, whose values can be extracted from (5.16) by separating out the terms dependent on $g^{\beta\mu}$ and $q^\beta\gamma^\mu$. This leads to

$$G_1 = 0 \qquad G_4 = -\frac{2}{\sqrt{3}}f_v\mathcal{I}_{D3}, \tag{5.17}$$

where the overlap integral $\mathcal{I}_{D3}$ is

$$\mathcal{I}_{D3} = \int_k b(\tilde{k},\tilde{q})\psi_\Delta^{D3}(P_+,k)\psi_N^S(P_-,k). \tag{5.18}$$

From Eqs. (3.14) and (3.15) we obtain

$$G_M^{D3}(Q^2) = -\frac{4}{3\sqrt{3}}\frac{m}{M+m}f_v\mathcal{I}_{D3}, \tag{5.19}$$

$$G_E^{D3}(Q^2) = -\frac{4}{3\sqrt{3}}\frac{m}{M+m}f_v\mathcal{I}_{D3}, \tag{5.20}$$

$$G_C^{D3}(Q^2) = 0. \tag{5.21}$$

Although formally different from the integral involved in the S-state transition, it can be shown that the integral $\mathcal{I}_{D3}$ goes with $1/Q^4$ for large Q^2. The proof follows the lines presented in case I of Appendix G in Ref. [68]. As a consequence, $G_M^{D3} = G_E^{D3}\sim 1/Q^4$.

2. Nucleon $(S) \to \Delta(D1)$

For the D1 transition the ρ term is no longer zero, and using Eq. (5.14), the property of the $S = 1/2$ projection operator, and the definition of $\mathcal{O}_2$ gives

$$\bar{\Gamma}^{\beta\mu}_{D1}(P,q)|_\rho = \sqrt{3} f_{2-} \int_k \Big\{ b(\tilde{k},\tilde{q}) q^\beta \frac{P^\mu}{m} \times \frac{1}{\tilde{q}^2} q^{\beta'} (\mathcal{P}_{1/2})_{\beta'\alpha} \gamma^\alpha \Big\} \psi^{D1}_\Delta \psi^S_N, \quad (5.22)$$

which contributes only to G_2

$$G_2|_\rho = -\frac{2\sqrt{3}M}{m d_-} f_{2-} \mathcal{I}_{D1}, \quad (5.23)$$

where the D1 overlap integral is

$$\mathcal{I}_{D1} = \int_k b(\tilde{k},\tilde{q}) \psi^{D1}_\Delta(P_+,k) \psi^S_N(P_-,k). \quad (5.24)$$

Comparing this calculation with Eq. (4.6), and using the connection $j_2 \to C_0 f_{2-}$, gives an explicit expression for $\rho_{(1/2)(1/2)}$

$$\rho_{(1/2)(1/2)}(Q^2) = \mathcal{R}_{(1/2)(1/2)} \frac{2M}{\sqrt{3} d_-} \mathcal{I}_{D1} = \frac{1}{3C_0} \sqrt{\frac{d_+}{2Mm}} \mathcal{I}_{D1}. \quad (5.25)$$

Next, using Eq. (5.15) for $S = 1/2$ case (where the $\gamma^\alpha \gamma^\mu$ term does not vanish), the $\mathcal{O}_1$ term for the D1 transition is

$$\bar{\Gamma}^{\beta\mu}_{D1}(P,q)|_{\mathcal{O}_1} = -\sqrt{3} f_v \int_k \Big\{ b(\tilde{k},\tilde{q}) \Big[\frac{q^\beta q^{\beta'}}{\tilde{q}^2} (\mathcal{P}_{1/2})_{\beta'\alpha} \Big] \times \Big(2 g^{\alpha\mu} - \gamma^\alpha \gamma^\mu - \frac{P^\alpha_- [2P^\mu_+ - 2M\gamma^\mu]}{mM + b} \Big) \Big\} \times \psi^{D1}_\Delta \psi^S_N. \quad (5.26)$$

From this we must extract the contributions to G_1, G_2, and G_4 [again ignoring G_3 which, using the modified current (4.13), will be given by the gauge invariant condition]. It is easy to see that $G_4 = 0$, and

$$G_1 = \frac{2M}{\sqrt{3} d_+} f_v \mathcal{I}_{D1} \qquad G_2|_{\mathcal{O}_1} = \frac{8M(2m+M)}{\sqrt{3} d_+ d_-} f_v \mathcal{I}_{D1}. \quad (5.27)$$

These contributions combine with (5.23) to give

$$G^{D1}_M(Q^2) = \frac{2}{3\sqrt{3}} \frac{m}{M+m} f_v \mathcal{I}_{D1}$$
$$G^{D1}_E(Q^2) = -\frac{2}{3\sqrt{3}} \frac{m}{M+m} f_v \mathcal{I}_{D1} \quad (5.28)$$
$$G^{D1}_C(Q^2) = \frac{4mM}{\sqrt{3} Q^2} f_C \mathcal{I}_{D1},$$

where f_C is the analogue of (4.9)

$$f_C = f_{1-} - \frac{Q^2}{2m(M+m)} f_{2-}. \quad (5.29)$$

Note that the expression (5.28) for $G^{D1}_C(Q^2)$ is consistent with (4.10) if we use the expression (5.25) and the connection $j_C \to C_0 f_C$.

Finally, as we have already discussed, the possible singularity in G^*_C must be canceled by imposing the requirement

$$\lim_{Q^2 \to 0} \mathcal{I}_{D1} \to A Q^2, \quad (5.30)$$

where A is a constant. This constraint predicts that the D1 contributions to the magnetic and electric form factors will be zero at $Q^2 = 0$. However, the constant A in the limit (5.30) will in general be nonzero, predicting that G^*_C is finite as $Q^2 \to 0$.

For large Q^2, we can write $\mathcal{I}_{D1}$ as a difference of two integrals of the type $\mathcal{I}_{D3}$ with different coefficients. Hence, $\mathcal{I}_{D1}$ goes like $1/Q^4$, which gives a $1/Q^4$ behavior for G^{D1}_M, G^{D1}_E and $G^{D1}_C \sim 1/Q^6$ (because $f_C \to$ constant as $Q^2 \to \infty$).

In the overall, the asymptotic expression for the form factors are consistent with pQCD [16].

C. Sum of all valence contributions

Considering the sum of all valence quark contributions, we obtain the contribution of the quark core, which we denominate by the "bare" (B) contribution

$$G^B_M(Q^2) = N[G^S_M + a G^{D3}_M + b G^{D1}_M], \quad (5.31)$$

$$G^B_E(Q^2) = N[a G^{D3}_M - b G^{D1}_M], \quad (5.32)$$

$$G^B_C(Q^2) = N b G^{D1}_C, \quad (5.33)$$

where we used the relations between the electrical and magnetic components for each state. Note that there are only two contributions for G^B_E, and one of them (G^{D1}_M) is zero for $Q^2 = 0$. As for G^B_C there is only the D1 state contribution.

For completeness we mention here that the nucleon could also have a D state. However, the nucleon (with total angular momentum $J = 1/2$) can only have the D state with core spin $3/2$. This nucleon D state can be built using the ideas presented in the previous sections and leads to an additional contribution to G^*_C. We have not considered such a D-state admixture in this paper because the nucleon form factors can be well described at low Q^2 [4] without including it.

VI. PION CLOUD CONTRIBUTION TO THE FORM FACTORS

The previous section presented the contribution for the form factors from the photon-quark interaction in relativistic impulse approximation, and within the spectator the-

ory. But the description of the electromagnetic $N\Delta$ transition requires also the presence of nonvalence degrees of freedom, which may involve two-body currents and/or sea quark contributions—dominated by virtual pion states, the pion cloud effects.

In the language of the dynamical models, where the hadronic interactions are described in terms of a baryon core that interacts with mesonic fields, a transition form factor can be separated into two terms [43,65,66]: the contribution of the quark core, or bare contribution, and the contribution from the pion cloud

$$G^*_\alpha(Q^2) = G^B_\alpha(Q^2) + G^\pi_\alpha(Q^2), \tag{6.1}$$

where α holds for M, E, C, and G^π_α denotes the corresponding mechanisms involving at least one intermediate pion state. This contribution is related with the long-range interaction, while G^B_α contains the short range physics [43] parametrized by the baryon wave functions. The decomposition (6.1) was also considered in Ref. [72].

Note that this scheme is model dependent, because the decomposition in background and resonances amplitudes is not unique [18,19,43,99]. However, once established the pion production mechanism (πNN amplitude), we can split G^*_α in two contributions in a given formalism.

Although our main goal here is the D-state effects in the core valence quark wave function, even a qualitative estimate of the D-state effects requires a simulation of the pion cloud effects. An effective parametrization of the pion cloud in G^*_M was already introduced in a previous work [68]. For G^*_E and G^*_C we consider in the present work the parametrization introduced in Refs. [24,53,70,71], which we will sketch now.

A. Pion cloud parametrization of G^*_C

In a pure SU(6) model the neutron electric form factor G_{En} would be identically zero and the multipoles E2 and C2 in the $\gamma N \to \Delta$ transition negligible. In the real world, G_{En} is small but nonzero.

Considering a constituent quark model with a confining harmonic oscillator potential with also pion- and gluon-exchange between quarks, Buchmann [53,72] concluded that the G_{En} data can be explained considering a two-quark current, with a quark-antiquark pair interacting with the external photon. In this description, the neutron spatial extension, expressed in term of its radius, can be written as

$$r_n^2 = -\frac{M^2 - m^2}{m} b_q^2, \tag{6.2}$$

where b_q is the quark core radius (oscillator parameter). For the experimental result, $r_n^2 \simeq -0.113$ fm^2, we can estimate $b_q \approx 0.6$ fm. Within the same formalism, one concludes [53] that

$$G^*_C(0) = -\sqrt{\frac{2m}{M}} Mm \frac{r_n^2}{6}. \tag{6.3}$$

As, for low Q^2, we can write for G_{En}

$$G_{En}(Q^2) \simeq -Q^2 \frac{r_n^2}{6}, \tag{6.4}$$

and we obtain, for small Q^2

$$G^*_C(Q^2) = \sqrt{\frac{2m}{M}} Mm \frac{G_{En}(Q^2)}{Q^2}. \tag{6.5}$$

The relation (6.5) can alternatively also be constructed from relations between the nucleon and nucleon to Δ transition magnetic moment, in the large N_c limit [24], for low Q^2 ($Q^2 \ll 1$ GeV^2).

Following Buchmann again, from a different perspective [72], the nucleon form factors can be described by a symmetric quark core distribution plus an asymmetric pion cloud around the inner core. Considering the proton electrical form factor, in particular, we can write

$$G_{Ep}(q^2) = G_{Ep'}(Q^2) + G^\pi_{Ep}(Q^2), \tag{6.6}$$

where $G_{Ep'}(Q^2)$ is the bare proton charge form factor, and $G^\pi_{Ep}(Q^2)$ is the contribution due to the pion cloud. In the same picture the neutron electric form factor is however just given by the pion cloud, and we may write

$$G_{En}(Q^2) = -G^\pi_{Ep}(Q^2), \tag{6.7}$$

since the charge distribution in the neutron bare core is zero. In the $Q^2 = 0$ limit, Eqs. (6.6) and (6.7) are directly related with the nucleon radii. From Eq. (6.4) we obtain $G_{En}(0) \sim r_n^2 \approx -0.113$ fm^2. As for G_{Ep}, we may write $G_{Ep}(Q^2) \simeq 1 - r_p^2 \frac{Q^2}{6}$, where r_p^2 is the proton electrical squared radius. Now, r_p^2 can be decomposed as $r_{p'}^2 - r_n^2 \approx 0.78$ fm^2, where $r_{p'}^2 \approx 0.67$ fm^2 represents the radius of the bare proton, the size of the proton being increased by the pion cloud.

As G_{En} is determined by pure pion cloud effects, we conclude that G^*_C (6.5) is the result of pion cloud effects (or equivalently, the Coulomb quadrupole form factor in the $\gamma N \to \Delta$ transition would be zero, for the case of no pion cloud effects). The previous derivation assumes no contribution from the inner core (symmetric distribution in the core). This assumption is not valid in general but can be a good approximation for a small D-state admixture. We will therefore use

$$G^\pi_C(Q^2) = \sqrt{\frac{2m}{M}} Mm \frac{G_{En}(Q^2)}{Q^2} \tag{6.8}$$

to represent the contribution of the pion cloud for G^*_C.

To check the consistency of this assumption, and before using it together with the bare model built here, we compare the R_{SM} data with the results extracted from the electrical form factor data using the parametrization (6.5). To estimate $G^*_M(Q^2)$ at the respective momentum Q^2, we consider the simple phenomenological parametrization of

Ref. [21]

$$G_M^*(Q^2) = 3G_D \exp(-0.21Q^2)\sqrt{1 + \frac{Q^2}{(M+m)^2}}. \quad (6.9)$$

The quality of this parametrization for G_M^* is presented in Fig. 3. The results are presented in Fig. 4, where we calculated G_{En} from our spectator constituent quark model. Although according to Eq. (6.5) the pion cloud contribution to G_C^* decreases with Q^2, its effect is not observed in the figure, due to the kinematic factor $\frac{|q|}{2M}$ present in R_{SM}.

Because of the nature of the derivation of Eq. (6.8) (large N_c limit and $Q^2 \sim 0$) we cannot say for sure whether or not the discrepancies in Fig. 4 are the result of the crude estimation ($\mathcal{O}(1/N_c^2)$ correction to the large N_c limit) or the result of neglecting the bare quark contribution. Reference [70] estimates the D-state effects from this one-body current to be 20% to the final result.

B. Pion cloud parametrization of G_E^*

Considering the large N_c limit, Pascalutsa and Vanderhaghen [24] related G_C^* and G_E^* at the photon point ($Q^2 = 0$)

$$G_C^*(0) = \frac{4M^2}{M^2 - m^2} G_E^*(0). \quad (6.10)$$

Using the relation (6.5) between G_C^* and G_{En}, and extending the results for finite Q^2, one has [24]

$$G_E^*(Q^2) = \left(\frac{m}{M}\right)^{3/2} \frac{M^2 - m^2}{2\sqrt{2}} \frac{G_{En}(Q^2)}{Q^2}. \quad (6.11)$$

This result was derived in Ref. [24], in the $Q^2 = 0$ limit, and must be restricted to low Q^2 ($Q^2 \ll 1$ GeV^2). The comparison between the R_{EM} data and the predictions from Eq. (6.11) using the G_{En} data is presented in Fig. 5.

In the G_C^* case, the exact SU(6) symmetry would imply $G_{En} \equiv 0$, and there is no contribution for the electric quadrupole. In contrast, one cannot conclude that Eq. (6.11) results uniquely from pure pion cloud effects. In the large N_c analysis, both G_E^* and G_C^* are $\mathcal{O}(1/N_c^2)$, to be compared with $G_M^* = \mathcal{O}(N_c^0)$, which is estimated in terms of the magnetic form factor of the neutron [65,72]. In that limit the valence quark core is dominant, but the next order correction can be originated by pion cloud effects or by angular momentum excitation of a quark. But, because G_E^* can be written in terms of r_n^2 (or $G_{En}(Q^2)$ for $Q^2 \sim 0$), we will take (6.11) as the pion cloud contribution for G_E^* for low Q^2, neglecting next order corrections $\mathcal{O}(1/N_c^3)$) in the large N_c limit

$$G_E^\pi(Q^2) = \left(\frac{m}{M}\right)^{3/2} \frac{M^2 - m^2}{2\sqrt{2}} \frac{G_{En}(Q^2)}{Q^2}. \quad (6.12)$$

Reference [53] estimates the contributions due to the quark-antiquark states G_E^π to be 88% of G_E^* for $Q^2 = 0$.

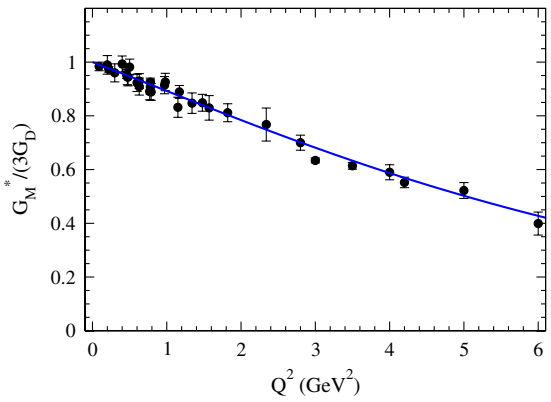

FIG. 3 (color online). Comparing the G_M^* data with the parametrization of Eq. (6.9).

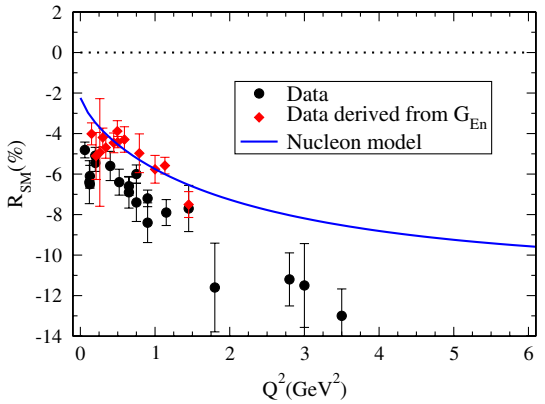

FIG. 4 (color online). Comparing the R_{SM} data with the prediction of Eq. (6.5) using the neutron electrical form factor data of Ref. [4]. The nucleon model line corresponds to the model of Ref. [4]. The nucleon wave function parameters are presented in Table I.

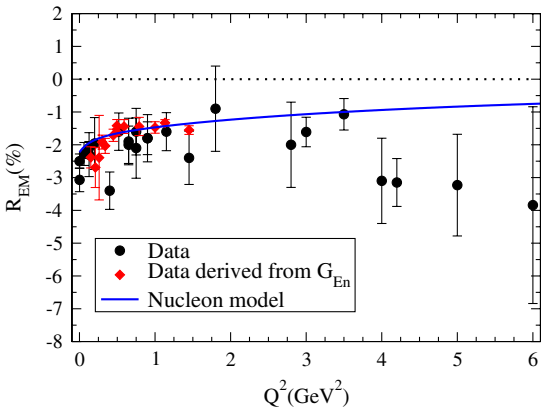

FIG. 5 (color online). Comparing the R_{EM} data with the prediction of Eq. (6.11) using the neutron electrical form factor data of Ref. [4]. The nucleon model line corresponds to the model of Ref. [4]. The nucleon wave function parameters are presented in Table I.

The relation between G_E^* and G_C^* represented in Eq. (6.10) is also known as the long wavelength limit for the ratio $G_C^*(0)/G_E^*(0)$). It is the result of the conditions $Q^2 \ll M^2 - m^2 \ll M^2, m^2$, like in the large N_c limit, where $M - m = \mathcal{O}(1/N_c)$. Equation (6.10) is also used to relate the electrical and Coulomb bare quadrupoles in the SL [43] and DMT [44] models.

A direct consequence of (6.10), if G_C^π and G_E^π are the only contribution for the respective form factors, is that [24]

$$R_{EM}(0) = R_{SM}(0). \tag{6.13}$$

Note that the pion cloud contributions (6.8) and (6.12) for G_C^* and G_E^*, respectively, go with $1/Q^6$ for large Q^2, competing with the bare contributions ($1/Q^6$ and $1/Q^4$, respectively). (Assuming as in Ref. [4] that $G_{En} \sim 1/Q^4$). As a consequence, the pion cloud contribution does not change the asymptotic behavior derived for G_E^B and G_B^C. We need to have in mind, however, that the results for G_C^π and G_E^π are derived under the assumption that Q^2 is small. Buchmann [71,72] argues that nevertheless, the pion cloud description for G_C^* can be extended also to the intermediate Q^2 region ($Q^2 \sim 4$ GeV^2).

With the parametrization of the pion cloud mechanisms using the Eqs. (6.8) and (6.12), we preserve the covariance of our calculation because G_{En} is evaluated using a spectator model [4].

VII. RESULTS

In this section, we present the numerical results of our model to the $\gamma N \to \Delta$ transition. For the quark current we adopted the quark form factors from Ref. [4] based on a vector dominance model parametrization

$$\begin{aligned} f_{1\pm}(Q^2) &= \lambda + \frac{(1-\lambda)}{1+Q^2/m_v^2} + \frac{c_\pm Q^2/M_h^2}{(1+Q^2/M_h^2)^2} \\ f_{2\pm}(Q^2) &= \kappa_\pm \left\{ \frac{d_\pm}{1+Q^2/m_v^2} + \frac{(1-d_\pm)}{1+Q^2/M_h^2} \right\}. \end{aligned} \tag{7.1}$$

In these expressions, m_v and M_h are the masses of the vectorial mesons. The lower mass $m_v = m_\rho$ (or m_ω), describes the two pion resonance (three pion resonance) effect, and M_h, fixed as $M_h = 2m$, takes into account all the larger mass resonances. The parameter λ was adjusted to give the correct quark density number in deep inelastic scattering [4,68]. All the other parameters are presented in Table I.

We will divide this section into two subsections. First we consider the effects of the valence quarks. In particular, we test whether the bare contributions alone calculated as explained in Sec. V can describe the experimental data. In the second subsection, we add the effects of the sea quarks (pion cloud effects), with the phenomenological, parameter free, description of the pion cloud presented in Sec. VI.

TABLE I. Parameters of the nucleon wave function (β_1, β_2) and quark form factors corresponding to the model II of Ref. [4]. In each case, we kept $\kappa_+ = 1.639$ and $\kappa_- = 1.823$ in order to reproduce the nucleon magnetic moments exactly.

β_1, β_2	c_+, c_-	d_+, d_-	λ, m_s/m
0.049	4.16	−0.686	1.21
0.717	1.16	−0.686	0.87

A. Valence quark contributions only: Models 1–3

With only valence quark degrees of freedom the $N\Delta$ electromagnetic transition form factors are described by Eqs. (5.31), (5.32), and (5.33). The free parameters of our model are the admixture coefficients a, b, and the momentum range parameters of the scalar wave functions (2.40) and (2.41). In a previous work, we adjusted the S-state Δ wave function to the G_M^* data considering also an effective pion cloud contribution [68] as

$$G_M^*(Q^2) = G_M^B(Q^2) + G_M^\pi(Q^2), \tag{7.2}$$

where G_M^B is the contribution of the quark core and G_M^π the pion cloud effects, parametrized by

$$G_M^\pi(Q^2) = \lambda_\pi \left(\frac{\Lambda_\pi^2}{\Lambda_\pi^2 + Q^2} \right)^2 (3G_D), \tag{7.3}$$

where $G_D = (1 + Q^2/0.71)^{-2}$ is the nucleon dipole form factor, Λ_π a cutoff, and λ_π a coefficient that defines the intensity of the pion cloud effect. The factor 3 was included for convenience: when $Q^2 = 0$, $G_M^\pi(0)/G_M^*(0) = \lambda_\pi$, then λ_π measures the fraction of pion cloud ($G_M^*(0) \approx 3$). The parametrization (7.3) simulates the main features of the pion cloud mechanism: significant contribution for $Q^2 = 0$; falloff with increasing Q^2. For more details see Ref. [68].

Here we extend the predictions to the subleading quadrupole form factors G_E^* and G_C^* expressed in the ratios R_{EM} and R_{SM} defined, respectively, by Eqs. (3.10) and (3.11). We kept the parametrization (7.2) and (7.3) for G_M^*; however, G_M^B is no longer determined only by the Δ S state, but now also includes contributions of both of the D states. For this reason the parameters originally fixed in the S state fit are now readjusted.

We considered the G_M^* data from CLAS/JLab [14,15], DESY [100], and SLAC [101]. For the electromagnetic ratios R_{EM} and R_{SM}, we use the data from MAMI [10,11], LEGS [12], MIT-Bates [13], and JLab [14,15]. Although there is no inconsistency in the G_M^* data, there is some ambiguity in the R_{EM} and R_{SM} data, dependent on the analysis. For the form factor information to be extracted one uses data for the pion photoproduction reaction cross sections. Those cross sections are interpreted in terms of an amplitude that includes a background and a resonant contribution. In the process, the extraction of the multipoles depends on assumptions for the background and resonance

parametrization. The multipole resonant amplitudes are then varied to fit the cross section data [18]. Kamalov *et al.* [45] presented a re-analysis of the CLAS-2002 data [14] with significant differences from the original data. Similarly, the CLAS-2006 R_{SM} data [15] for $Q^2 \geq 3$ GeV^2 shows a dependence on Q^2 different from the recent MAID analysis [75] of the same data. The R_{EM} analysis from Arndt *et al.* [102] is in contradiction with all the published results. More recently, Stave [67] showed that there is significant discrepancies in the extraction of E2 and C2 from the data using different reaction models like SL and DMT in the region $Q^2 < 1$ GeV^2. (This discrepancy can be reduced by refitting the models within the range $Q^2 < 1$ GeV^2 only, which however prevents the range of the application of the models for higher Q^2 regions.)

As a first step, model 1 fits only the G_M^* and R_{EM} data (using, as in Ref. [68], the bare data extracted by the SL model [43] to constrain the bare form factor G_M^B). This fit (together with the fit from model 2 described below) is shown in Fig. 6. The Coulomb form factor predicted by model 1 (and not used in the fit) is shown in Fig. 7.

The parameters that were adjusted during the fits are shown in Table II. Although we did not fit the R_{SM} data, the coefficient b, which determines the strength of the D1 state, was adjusted during the fit. (As emphasized in the previous sections, only the D1 state can generate a non-vanishing R_{SM}, or $G_C^* \neq 0$.) As we see in Table II, the best description of the G_M^* and R_{EM} data requires a small admixture of the D1 state (0.2%). To check the sensitivity of the fit to the inclusion of the D1 state, we considered also another fit forcing $b = 0$. This defines model 2. As Table II shows, the admixture with $b \neq 0$ improves the description of the data only slightly (χ^2 of 2.72 versus 2.83), meaning that the role of the D1 state is not decisive for G_M^* and R_{EM}.

Figure 7 shows the prediction of model 1 for R_{SM} (the result for model 2 is zero). We conclude that the R_{SM} prediction from model 1 is an order of magnitude smaller than the data.

The next step is to try to fit the R_{SM} data as well, still using only the valence quark degrees of freedom. However, because of the zero in f_C, Eq. (5.29), we also predict a zero in G_C^*, Eq. (5.28). Using the parameters of Ref. [4], f_C passes through zero around $Q^2 \simeq 5.6$ GeV^2. This zero is completely at odds with the data. It is therefore impossible to fit G_C^* over the entire Q^2 range, and at this stage we restrict the fit to R_{SM} to the low momentum region $Q^2 < 1.5$ GeV^2. This fit defines model 3.

The results from model 3 are shown in Fig. 8. In the last panel of the figure we show R_{SM} for $Q^2 < 1.5$ GeV^2 only, the range used in the fit. Figure 7 compares the results for R_{SM} obtained from models 1 and 3 over the entire Q^2 range. Note the unavoidable zero for model 3 at $Q^2 \sim 5.6$ GeV^2. The first conclusion from model 3 is that the fit gives R_{SM} only within the region $Q^2 < 1.5$ GeV^2, and that the fit is a poor one (high χ^2_{RSM}). Also, the quality of the description of the G_M^* data is affected, as we can conclude from Table II, by comparing χ^2_{GM} obtained in model 3 with the corresponding values obtained in models

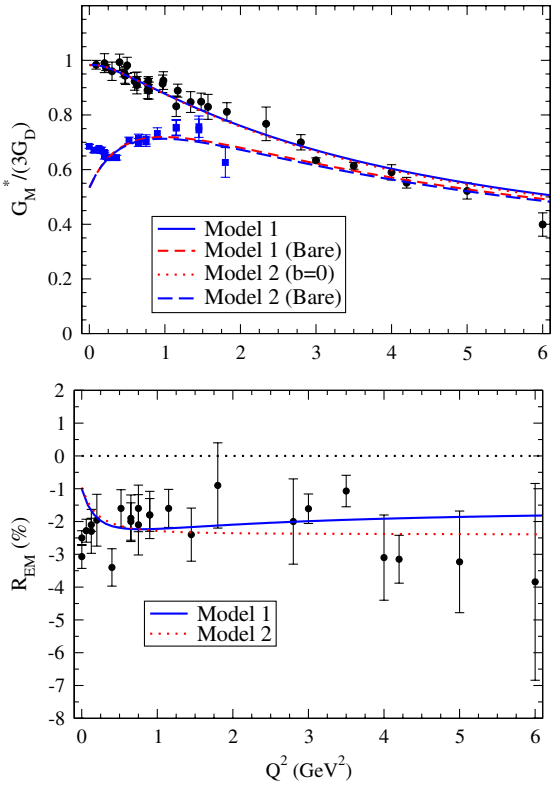

FIG. 6 (color online). Models 1 and 2. G_M^* data from CLAS/JLab [14,15], DESY [100] and SLAC [101]. R_{EM} data from MAMI [10,11], LEGS [12], MIT-Bates [13], and JLab [14,15]. The bare data for G_M^B, shown in the top panel, were extracted from the SL analysis, Ref. [43]. For the fit we doubled the bare data error bars shown in the figure to constrain G_M^B, but the extra χ^2 that results from the fit of G_M^B to bare data is not included in any of the χ^2 reported in this paper.

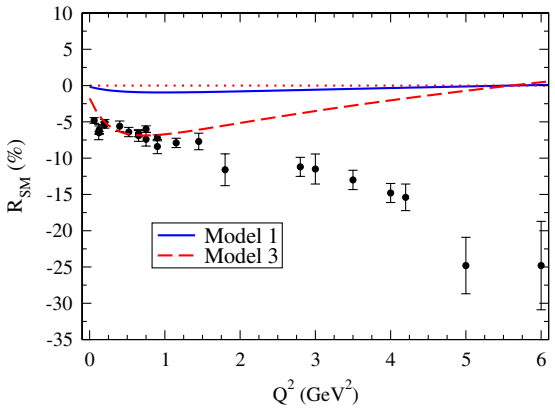

FIG. 7 (color online). R_{SM} from models 1 and 3. Data from MAMI [10,11], LEGS [12], MIT-Bates [13], and JLab [14,15].

TABLE II. Model 1 fits G_M^* and R_{EM}. Model 2 fits the same quantities with $b = 0$ (no D1 mixture). Model 3 fits all variables but restricts $Q^2 < 1.5$ GeV^2 for R_{SM}. Model 4 includes an effective pion cloud in both R_{EM} and R_{SM} (for $Q^2 < 4.3$ GeV^2). All models also fit G_M^B to the bare data (as shown in the figures) but the extra χ^2 that results from the fit to bare data is not included in the χ^2 reported in the last two columns.

Model	λ_π, Λ_π^2	α_1, α_2	α_3, α_4	λ_{D1}, α_5	D3, D1	χ^2_{GM}, χ^2_{REM}	χ^2_{RSM}, χ^2
1	0.450	0.344	0.1956	1.025	8.15%	1.41	—
	1.46	0.344	0.1978	0.1165	0.17%	4.39	**2.72**
2	0.448	0.350	—	—	8.16%	1.21	—
	1.53	0.343	—	0.0991	—	4.90	**2.83**
3	0.479	0.343	0.1567	1.0087	8.50%	3.33	11.84
	1.30	0.350	0.1574	0.2218	15.2%	3.80	**5.45**
4	0.441	0.336	0.1089	1.0094	0.88%	1.41	5.68
	1.53	0.337	0.1094	0.1880	4.36%	0.99	**2.51**

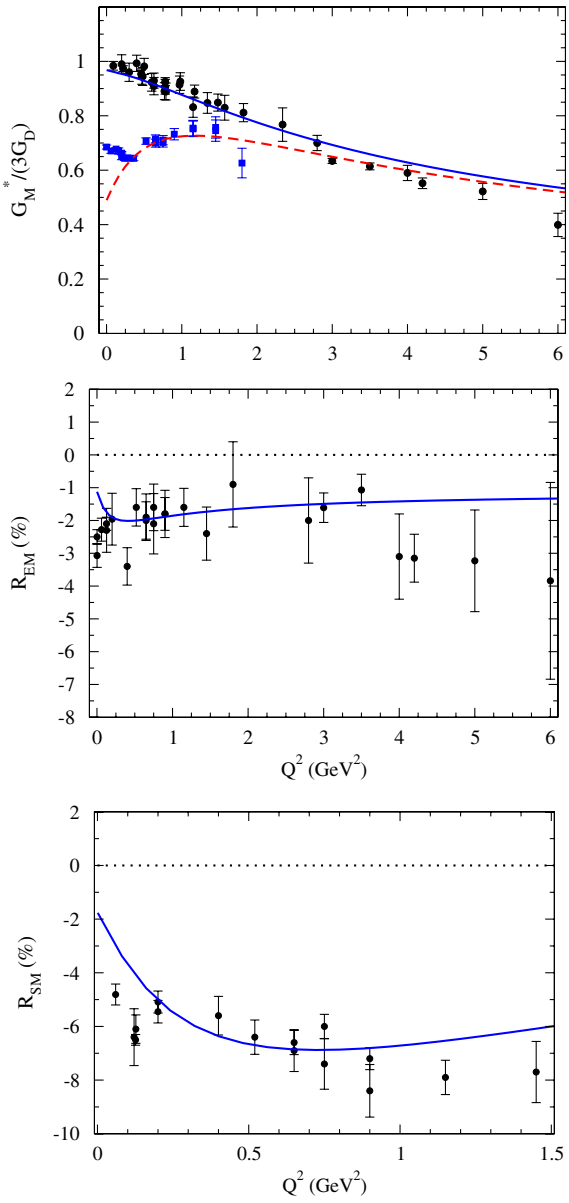

FIG. 8 (color online). Model 3. Data from Figs. 6 and 7.

1 and 2. Note also that even the qualitative description of R_{SM} provided by model 3 requires an abnormally large admixture of the D1 states (15.2%). All these observations show the intrinsic limitations of a pure constituent quark model. They can be overcome by adding pion cloud effects, as motivated in the discussion in the previous section.

At low Q^2, the data tell us that $R_{SM}(0) \approx -4\%$, which is equivalent to $G_C^*(0) \approx 1.1$ [this follows from (3.11) with $G_M^*(0) \simeq 3$]. Without a pion cloud such a result can be obtained in this formalism only by requiring a large D1 admixture. But even with a large D1 admixture, the valence quark contribution for R_{SM} changes sign at about $Q^2 \sim 5.6$ GeV^2, and we are led to conclude that the valence quark degrees of freedom are insufficient to explain the G_C^* data for large Q^2. This conclusion is consistent with both constituent quark models and the results from dynamical models.

Let us discuss now the numerical values of the range parameters α_i. Remember that α_i can be interpreted as a Yukawa range parameter [4,6], with a smaller α parameter representing a larger spatial range. It is interesting to see that in all the models with D-state components, $\alpha_1 \simeq \alpha_2$. This finding differs from the results obtained previously for a Δ wave function with only an S-wave component [68]. For the pure S state, $\alpha_1 \approx 0.3$ and $\alpha_2 \approx 0.4$. Apparently, the introduction of the D states sets a new long-range scale, with $\alpha_i \sim 0.1$ to 0.2, for $i = 3, 4, 5$. These longer range scales are also nicely consistent with the notion that the D waves are peripheral. Finally, it is worth mentioning that the similarity in the values for α_1, $\alpha_2 \simeq 0.35$, suggests that the S-state effects are somehow model independent. This feature suggests that, in the future, it might suffice to chose only 1 parameter to describe the S state of the Δ, showing that the improvement that accompanies the inclusion of the D-states is robust.

Summarizing: a qualitative description of the G_M^* and G_E^* data can be obtained using a Δ wave function composed predominantly of an S state with admixtures of D3 and D1 states. A fit based on a quark core requires an 8.2% admixture of the D3 state. The inclusion of the D1 state is

not at all necessary to explain the G_M^* and G_E^* data. To explain the G_C^* data using only a quark core requires an unusual large admixture of the D1 state, and is only reasonable for low Q^2, failing totally for $Q^2 > 2$ GeV^2 (see Fig. 7). The conclusion from models 1–3 is that a quark core only is not sufficient to explain the $\gamma N \to \Delta$ transition data, even when the Δ wave function includes admixtures of D1 and D3 states.

B. A mixed description: valence quarks and a pion cloud: Model 4

We now add a pion cloud contribution to the G_E^* and G_C^* form factors

$$G_E^*(Q^2) = G_E^B(Q^2) + G_E^\pi(Q^2)$$
$$G_C^*(Q^2) = G_C^B(Q^2) + G_C^\pi(Q^2), \tag{7.4}$$

where the pion cloud contributions are taken from Eq. (6.12) and Eq. (6.8), respectively. There are no adjustable parameters in the pion cloud components. For the neutron electric form factor $G_{En}(Q^2)$ we use model II of Ref. [4] (see Table I). The limit of validity of the pion cloud formulas is restricted to low Q^2, which led us to restrict our fit to R_{SM} to the $Q^2 < 4.3$ GeV^2 region. The bare contributions from valence quarks come from (5.32) and (5.33). Then, G_E^B is the result of the valence quark contribution involving the D3 and D1 states, and G_C^B comes only from the D1 state.

The results for model 4: the fit obtained using the pion cloud, are shown in Fig. 9, with the parameters given in Table II (along with the results for all the other models). The description of G_C^* (and the corresponding ratio R_{SM}) by model 4 for $Q^2 > 2$ GeV^2 favors the recent MAID analysis [75] over the original JLab analysis [15], and its success or failure will ultimately depend on which of these analysis survives further study.

By comparing the χ^2s in Table II for models 3 and 4, one concludes that the inclusion of the pion cloud for G_E^* and G_C^* does indeed improve significantly the simultaneous description of the data of these two more problematic observables. In model 4, the contribution of the pion cloud at $Q^2 = 0$ is 86.9% for G_E^*, and 72.5% for G_C^*. The most important D state is the D1, with a small admixture of 4.4% compared with a tiny admixture of a D3 state of only 0.9%. As for the dominant G_M^* form factor, the pion cloud contribution estimated using an S-wave model does not change with the inclusion of D waves (44.1% for model 4 to be compared with 46.4% from Ref. [68]). The magnitude of the cutoff, Λ_π^2, in the pion cloud contribution to G_M^* is decreased slightly (1.53 GeV^2 versus 1.22 GeV^2). The addition of the pion clouds term to the D-wave states does not change the previously observed approximate equality $\alpha_1 \simeq \alpha_2$, although it reduces very slightly the value of these range parameters.

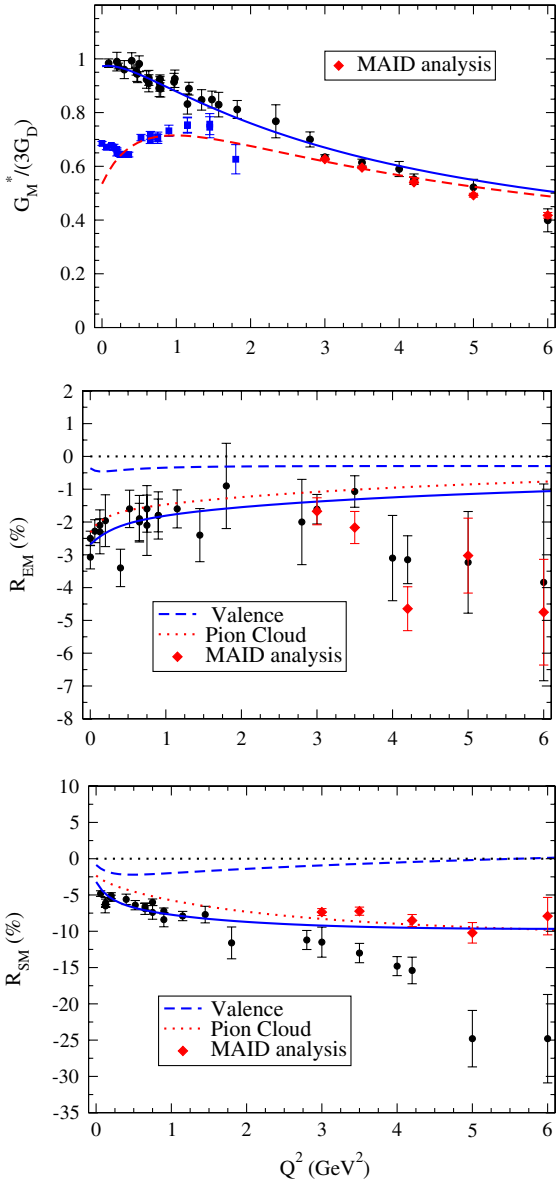

FIG. 9 (color online). Model 4. Data from Figs. 6 and 7, and the recent MAID analysis [75].

Even though the pion cloud contributions dominate the description of the small form factors, our model suggests that the corrections coming from the valence quark sector are still important to obtain the best description of the data. This can be confirmed in Fig. 9, in particular, for R_{SM}. Leaving aside the discrepancy at high Q^2, which depends on the resolution of the differences between the recent MAID analysis and the older JLab analysis. The figure shows that the pion cloud contribution, which in our work is parameter free, underestimates the data.

While model 4 fits the overall data well, and is clearly the best model found, there are at least three ways in which our theory and the experimental data could be improved. First, the validity of our model for the pion cloud can be

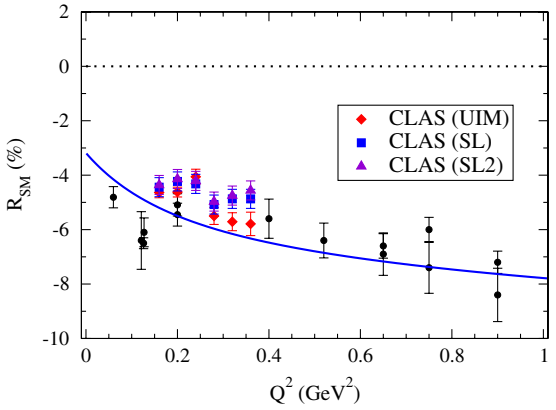

FIG. 10 (color online). R_{SM} from model 4 with data and preliminary CLAS data using a unitary isobar model, SL model from [41] and [43] (SL2). The preliminary CLAS data was not used in the fit.

questioned, particularly away from the photon point, $Q^2 = 0$. Second, the analysis of the data for $Q^2 < 0.15\,\mathrm{GeV}^2$ and for large Q^2 is uncertain. If the low Q^2 data is excluded from the fit, we found that a higher quality description of R_{SM} was possible, with $\chi^2 \sim 1.2$. That there is some legitimacy in excluding this data may be seen from a comparison between different data sets, shown in Fig. 10. The experiments for $Q^2 = 0.121\,\mathrm{GeV}^2$ from MIT-Bates and $Q^2 = 0.126, 0.127\,\mathrm{GeV}^2$ from MAMI suggest a large negative fraction for the R_{SM} (around -7%), in contradiction with the data for $Q^2 = 0.2\,\mathrm{GeV}^2$ GeV^2 from MAMI, and also the very recent preliminary CLAS data [43,67,84] ($R_{SM} \sim -5\%$). The final analysis of the CLAS data should clarify this point.

Finally, our treatment of the valence quark sector can be questioned. The factor f_C in Eq. (5.29) gives a zero in G_C^B, which implies a dominance of the pion cloud for $Q^2 \sim 6\,\mathrm{GeV}^2$. To study the model dependence on this behavior of f_C, we probed a change in the quark anomalous magnetic moments $\kappa_\pm$. We tried to suppress the large Q^2 behavior of f_{2-} by redefining $\kappa_\pm \to \kappa_\pm \frac{\Lambda^2}{\Lambda^2+Q^2}$, with Λ an adjustable cutoff. This reparameterization decreased the overall χ^2 obtained for the description of the transition data, but also increased the χ^2 for the fit to the nucleon form factor data. Clearly, this effect deserves more study.

VIII. COMPARISON WITH OTHER WORKS

In general, our results agree qualitatively with Refs. [53,70] and support the general idea that the quadrupole transition form factors are dominated by pion cloud effects [19,27,44,65–67] or quark-antiquark states [53,70–72]. In particular, our pion cloud contribution is consistent with both chiral perturbation and lattice QCD estimations.

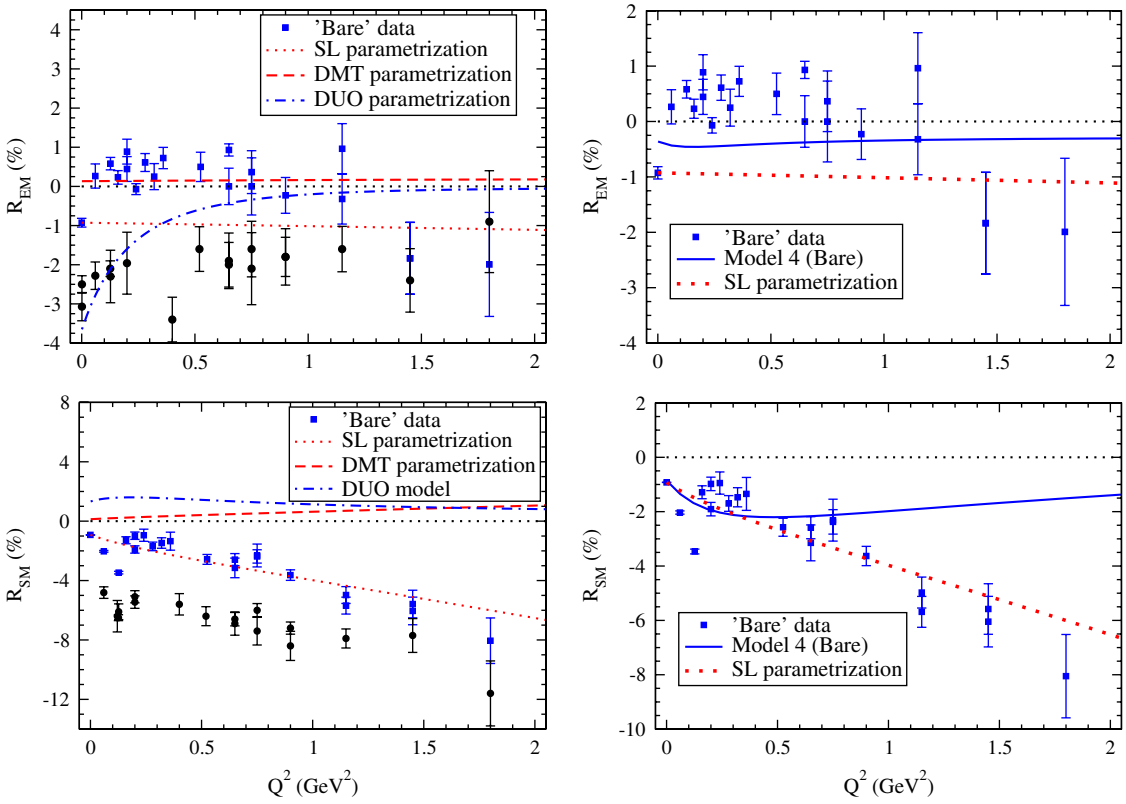

FIG. 11 (color online). Left side: Parametrization to the bare form factors from SL [41], DMT [44,45], and DUO [46] models. The circles represent the experimental data from Figs. 6 and 7. Right side: Model 4 compared with SL and bare data. The ratios were evaluated using the parametrization of G_M^* from (6.9). In both cases the bare data is from Ref. [43].

TABLE III. Bare contribution in different models, estimated by subtraction of the pion cloud. In the lines labeled with an "*", the total result was not available and model 4 was used.

$Q^2 = 0$ GeV^2	G_E^B/G_E^*	G_C^B/G_C^*
DMT [73]	−5.7%	−4.7%
SL [73]	33%	36%
DUO*	136%	−42%
Buchmann [53,70]	12%	20%
Model 4	13%	18%
$Q^2 = 1$ GeV^2	G_E^B/G_E^*	G_C^B/G_C^*
DMT*	−8.8%	−8.2%
SL*	56%	51%
DUO*	11%	−15%
Model 4	17%	18%

Also, according to results of chiral perturbation theory $R_{SM} \sim \log m_\pi$ as $m_\pi \to 0$, which implies significant pion cloud effects at the physical pion mass [20,21,103]. Additionally, the EFT calculations of Gail *et al.* [21,73] predict a dominance of the pion cloud effects. The recent quenched and unquenched lattice QCD calculations [64] for pion masses $m_\pi > 0.35$ GeV predict only a small fraction of the experimental result for G_C^* for low Q^2. This fact suggests as well that the pion cloud effects are dominant in G_C^* for low Q^2 (the enhancement of the chiral loop corrections relative to lattice data for small pion masses was shown in Ref. [20]).

Constituent quark models, such as the Isgur-Karl model [28,65], include S states and a D-state admixture of typically 1%, but predict only a fraction of the total G_E^* and G_C^* near $Q^2 = 0$. This feature is also shared by several relativistic quark models [30,32] and by the valence contribution of our model 4 (see Figs. 9 and 11). The exception to this role is the work of Ref. [52], where a manifestly Lorentz covariant chiral quark approach was considered. In that work the effect of the pion cloud is reduced to the order of 10%, which is compensated by a significant contribution of relativistic effects when compared with nonrelativistic quark models. A discussion of the predictions of quark models for low Q^2 can be found in Refs. [11,27,65,67].

We conclude this section by looking at the implications of describing the pion cloud with a DM. Dynamical models assume that the complete electroproduction (or photoproduction) amplitude is the iteration of a kernel composed of the sum of bare resonance pole(s) in the s channel, plus "left-hand cuts" (arising from the angular average of t and u channel poles coming from the exchanges of mesons and baryons). Fitting the data with such a model fixes *both* the bare resonance parameters *and* the parameters of the left-hand cuts, which dynamically determine the background, and in this way allows one to extract bare "data," or that part of the form factors that would be present even without the dressing produced by the rescattering of pions. Predictions of a pure CQM could be compared directly with this bare data, since both exclude the same physics—all pion rescattering mechanisms.

The bare data extracted from the fits of Ref. [43] are compared with various theoretical models in Fig. 11. Since the comparison involves electromagnetic ratios and not absolute quantities, we used (7.2) to parametrize G_M^*, which is present in all the ratios shown in the figure. The left-hand panels show the comparison of bare data to the parametrizations used by SL [41], DMT [44,45], and the dynamical Utrecht-Ohio (DUO) [46] models. Note that there is a substantial difference between the bare data [43] and the parametrization initially used in the SL model [41], particularly for R_{EM}.

The figure eloquently exhibits that bare contributions are strongly model dependent, in their size and even their sign, differing from model to model. All that we can conclude from these results, considering also the observed experimental data, is that bare contributions and pion cloud contributions are both sizable (see Table III). The exception is the DMT model, where the bare contributions are almost negligible for low Q^2 ($\sim 5\%$). As for the SL model [41], the bare contribution is 33% and 36% for E2 and C2, respectively, at $Q^2 = 0$ [73] (corresponding to a pion cloud contribution of 77% for E2 and 74% for C2 at the photon point). A compilation of the bare contribution for E2 and C2 for different models is presented in Table III for $Q^2 = 0$ and $Q^2 = 1$ GeV^2. For a summary of the literature see also Refs. [65,73,74].

IX. CONCLUSIONS

In this work we introduce for the first time the D states in the covariant spectator formalism for the description of baryons as a quark-diquark systems, and apply our formalism to the description of the form factors of the electromagnetic $N\Delta$ transition. Covariant formalisms provide a correct treatment of boosts and rotations, which are important to describe correctly the kinematics and the dynamics in the intermediate Q^2 region ($Q^2 \sim 4$ GeV^2). There are two D states for the Δ: one for the valence quark core of spin 3/2 (D3 state), the other for valence core of spin 1/2 (D1 state). We show that these D states have the correct spin structure in the baryon rest frame. Within this framework, we show here that a consistent model, with orthogonal nucleon and Δ wave functions, predicts nonvanishing contributions for the electric and Coulomb quadrupole form factors, an indirect signature of the asymmetry of the valence quark distribution in space.

However, we start by finding that the D-state contributions are not enough to explain the experimental data for G_E^* and G_C^*. An admixture of an 8% D3 state can explain the R_{EM} data, but the R_{SM} data cannot be explained without a D1 component. Importantly, although, is that even a very large admixture of the D1 state cannot explain the high Q^2

behavior of this observable. This conclusion is consistent with results from other constituent quark models in the literature.

With this established, we had to turn our attention to the pion cloud effects. We find that the pion cloud contributions are essential to an accurate description of the $\gamma N \to \Delta$ transition, and that our best model (model 4) gives a good overall description of the $\gamma N \to \Delta$ transition form factors. In this model, we used pion cloud effects derived in the large N_c limit, containing no adjustable parameters, and our fit predicts that the Δ wave function is the sum of a large S-state component with an admixture of 0.9% for the D3 state and a reasonable 4.4% weight for the D1 state. The pion cloud dominants G_E^* and G_C^*, with contributions of 87% and 73%, respectively, at the photon point. Like the valence quark contribution, the pion cloud contribution is also covariant because it is based on a covariant description of the neutron electric form factor. As the pion cloud parametrization presented here can be justified only for low Q^2 ($Q^2 < 1.5$ GeV^2, in accordance with Ref. [24]), in the future we are planing to include an explicit relativistic calculation of the pion cloud, to replace the effective parametrization.

The momentum distribution of the D3 state is determined by one parameter ($\alpha_5 \simeq 0.20$), and that of the D1 state by two parameters, which turn out to be nearly equal ($\alpha_3 \simeq \alpha_4 \simeq 0.10$). These values are smaller than the one parameter ($\alpha_1 \simeq \alpha_2 \simeq 0.35$) required to represent the S state, consistent with the picture that the D waves are more peripheral.

We conclude with two notes which concern also future developments:

(1) We found that the quality of the description of the data is very sensitive in the regions $Q^2 < 0.2$ GeV^2 and at higher $Q^2 > 3$ GeV^2. Evidence for problems in the data come from an apparent inconsistency between the G_C^* data for $Q^2 \simeq 0.13$ GeV^2 and $Q^2 \simeq 0.2$ GeV^2. The new CLAS data [43,67,84] for $0.16\ \text{GeV}^2 \leq Q^2 \leq 0.34\ \text{GeV}^2$ can be useful to clarify the situation. For high Q^2, the understanding of the differences between the CLAS analysis and the MAID analysis will be also crucial for future progress.

(2) Presumably the most accurate estimate of the pion cloud effects comes from dynamical models that compute the dressing of the bare quark currents by pion rescattering to all orders. As a by-product, these dynamical models determine the parameters of the valence, or undressed, quark contribution, which can be compared with a quark model without pion cloud effects. We observed that the results from the bare, pure valence quark form factors strongly depend on the pion production model (see SL, DMT, or DUO models presented in the text). It becomes therefore crucial to use valence quark models to estimate directly the bare form factors as functions of Q^2, and to understand the nature of the valence quark distribution in the nucleon and Δ system, as we do here. Since the valence quark distribution dominates the largest $\gamma N \to \Delta$ transition form factor G_M^* [68], dynamical models should use valence quark models as input, instead of relying on phenomenological parameterizations.

ACKNOWLEDGMENTS

G. R. wants to thank Vadim Guzey, José Goity, and Kazuo Tsushima for the helpful discussions. The authors want also to thank to B. Juliá Díaz for sharing the "bare data" of Ref. [43]. This work was partially support by Jefferson Science Associates, LLC under U.S. DOE Contract No. DE-AC05-06OR23177. G. R. was supported by the Portuguese Fundação para a Ciência e Tecnologia (FCT) under Grant No. SFRH/BPD/26886/2006.

APPENDIX A: SPIN STRUCTURE OF THE D-WAVE MATRIX ELEMENTS

In this appendix we first show how the spin 3/2 function $V_{3/2}$ [defined in Eq. (2.35)] satisfies the special spin 3/2 constraint

$$\gamma_\alpha V^\alpha_{3/2}(P, \lambda) = 0 \tag{A1}$$

and then prove the relations (2.36) and explicitly construct the matrix elements in the expansions (2.37).

To show that $V_{3/2}$ satisfies the special spin 3/2 condition, go to the rest frame $\bar{P} = (M, 0, 0, 0)$ and observe that

$$\gamma_\alpha V^\alpha_S(\bar{P}, \lambda_s) = \sum_\lambda \begin{pmatrix} 0 & -a_{\lambda_s\lambda} \\ a_{\lambda_s\lambda} & 0 \end{pmatrix} \begin{bmatrix} \chi_\lambda \\ 0 \end{bmatrix}, \tag{A2}$$

where the 2×2 operator is

$$a_{\lambda_s\lambda} = \left\langle \frac{1}{2}\lambda 1\lambda' \middle| \frac{3}{2}\lambda_s \right\rangle \sigma_{\lambda'}, \tag{A3}$$

with

$$\sigma_\lambda = \sigma_i \varepsilon^i_\lambda = \begin{cases} \sigma_z & \lambda = 0 \\ \begin{pmatrix} 0 & -\sqrt{2} \\ 0 & 0 \end{pmatrix} & \lambda = 1 \\ \begin{pmatrix} 0 & 0 \\ \sqrt{2} & 0 \end{pmatrix} & \lambda = -1 \end{cases}. \tag{A4}$$

Examining the $\lambda_s > 0$ cases shows that

$$\begin{aligned} \sum_\lambda (a_{3/2\lambda})\chi_\lambda &= \sigma_1 \chi_+ = 0 \\ \sum_\lambda (a_{1/2\lambda})\chi_\lambda &= \sqrt{\frac{2}{3}}\sigma_0 \chi_+ + \sqrt{\frac{1}{3}}\sigma_1 \chi_- = 0. \end{aligned} \tag{A5}$$

Similar results hold for the $\lambda_s < 0$ cases.

The orthogonality and normalization relations (2.36) follow immediately from the orthogonality and normalization of the spinors and polarization vectors, and the unitarity of the CG coefficient matrix. The completeness relations follow from the normalization and orthogonality relations, but it is instructive to prove them directly. To do this go to the rest frame and compute the matrix elements of the projectors in the spherical basis. Define

$$P^S_{\lambda\lambda'} = \varepsilon^{\alpha *}_{\lambda P}(\mathcal{P}_S)_{\alpha\beta}\varepsilon^{\beta}_{\lambda' P} \tag{A6}$$

and note that this matrix is Hermitian and when multiplied by the projection operator $(M + \bar{\not{P}})/(2M) = \frac{1}{2}(1 + \gamma^0)$ is of the block diagonal form

$$P^S_{\lambda\lambda'} = \begin{pmatrix} -p^S_{\lambda\lambda'} & 0 \\ 0 & 0 \end{pmatrix}, \tag{A7}$$

where the 2×2 submatrices have the symmetry property

$$\sigma_x p^S_{\lambda\lambda'}\sigma_x = p^S_{-\lambda-\lambda'}. \tag{A8}$$

Hence, there are only three independent elements, which will be chosen to be p_{00}, p_{11}, and p_{01}. Using the definitions of the projection operators (2.25), in the rest frame we obtain directly

$$\begin{aligned} p^{1/2}_{00} &= \frac{1}{3}\begin{bmatrix} 1 & 0 \\ 0 & 1 \end{bmatrix} \qquad p^{3/2}_{00} = \frac{2}{3}\begin{bmatrix} 1 & 0 \\ 0 & 1 \end{bmatrix} \\ p^{1/2}_{11} &= \frac{1}{3}\begin{bmatrix} 0 & 0 \\ 0 & 2 \end{bmatrix} \qquad p^{3/2}_{11} = \frac{1}{3}\begin{bmatrix} 3 & 0 \\ 0 & 1 \end{bmatrix} \\ p^{1/2}_{10} &= -\frac{1}{3}\begin{bmatrix} 0 & \sqrt{2} \\ 0 & 0 \end{bmatrix} \qquad p^{3/2}_{10} = \frac{1}{3}\begin{bmatrix} 0 & \sqrt{2} \\ 0 & 0 \end{bmatrix}. \end{aligned} \tag{A9}$$

These same operators can be calculated from the definitions (2.35) and the expansions (2.36). In the rest system the spherical components of these expansions are

$$\begin{aligned} \mathcal{O}^S_{\lambda\lambda'} &\equiv \sum_{\lambda_s} \varepsilon^{\alpha *}_{\lambda\bar{P}} V_{S\alpha}(\bar{P}, \lambda_s)\bar{V}^{\beta}_S(\bar{P}, \lambda_s)\varepsilon^{\beta}_{\lambda'\bar{P}} \\ &= \sum_{\lambda_s}\left\langle \frac{1}{2}\lambda_1 1\lambda \,\middle|\, S\lambda_s\right\rangle\left\langle \frac{1}{2}\lambda'_1 1\lambda' \,\middle|\, S\lambda_s\right\rangle \\ &\quad \times u_\Delta(\bar{P}, \lambda_1)\bar{u}_\Delta(\bar{P}, \lambda'_1), \end{aligned} \tag{A10}$$

where the operator $\mathcal{O}$ has the form

$$\mathcal{O}^S_{\lambda\lambda'} = \begin{pmatrix} -o^S_{\lambda\lambda'} & 0 \\ 0 & 0 \end{pmatrix}, \tag{A11}$$

with the 2×2 matrix

$$o^S_{\lambda\lambda'} = \sum_{\lambda_s}\left\langle \frac{1}{2}\lambda_1 1\lambda \,\middle|\, S\lambda_s\right\rangle\left\langle \frac{1}{2}\lambda'_1 1\lambda' \,\middle|\, S\lambda_s\right\rangle \chi_{\lambda_1}\chi^{\dagger}_{\lambda'_1}. \tag{A12}$$

This operator has the same symmetry properties as $p^S_{\lambda\lambda'}$, and by explicit computation

$$\begin{aligned} o^S_{00} &= \left[\left\langle \frac{1}{2}\frac{1}{2}10 \,\middle|\, S\frac{1}{2}\right\rangle\right]^2\begin{pmatrix} 1 & 0 \\ 0 & 0 \end{pmatrix} \\ &\quad + \left[\left\langle \frac{1}{2}-\frac{1}{2}10 \,\middle|\, S-\frac{1}{2}\right\rangle\right]^2\begin{pmatrix} 0 & 0 \\ 0 & 1 \end{pmatrix} \\ &= \begin{cases} \frac{1}{3}\begin{pmatrix} 1 & 0 \\ 0 & 1 \end{pmatrix} & S = \frac{1}{2} \\ \frac{2}{3}\begin{pmatrix} 1 & 0 \\ 0 & 1 \end{pmatrix} & S = \frac{3}{2} \end{cases} \end{aligned} \tag{A13}$$

in agreement with Eq. (A9). Similar agreement is obtained for the other matrices.

We now turn to the computation of the matrix elements in Eq. (2.37). Using the direct product representations (2.35) (and a similar one for w_γ)

$$\begin{aligned} C_{D2S} &\equiv \bar{V}_{S\alpha}(P, \lambda_s)\mathcal{D}^{\alpha\gamma}w_\gamma(P, \lambda_\Delta) \\ &= \sum_\lambda \left\langle \frac{1}{2}\lambda 1 m \,\middle|\, S\lambda_s\right\rangle\left\langle \frac{1}{2}\lambda 1 m' \,\middle|\, \frac{3}{2}\lambda_\Delta\right\rangle D_{mm'} \\ &= \frac{1}{3}\sqrt{8\pi}\mathbf{k}^2 Y^2_{m_\ell}\sum_\lambda \langle 2m_\ell 1m|1m'\rangle \\ &\quad \times \left\langle 1m'\frac{1}{2}\lambda \,\middle|\, \frac{3}{2}\lambda_\Delta\right\rangle\left\langle 1m\frac{1}{2}\lambda \,\middle|\, S\lambda_s\right\rangle, \end{aligned} \tag{A14}$$

where the CG coefficients guarantee that $m = \lambda_s - \lambda$, $m' = \lambda_\Delta - \lambda$, and $m_\ell = m' - m = \lambda_\Delta - \lambda_s$. The sum over three CG coefficients is evaluated using Racah coefficients W. For the cases at hand [104],

$$\begin{aligned} &\sum_\lambda \langle 2m_\ell 1m|1m'\rangle\left\langle 1m'\frac{1}{2}\lambda \,\middle|\, \frac{3}{2}\lambda_\Delta\right\rangle\left\langle 1m\frac{1}{2}\lambda \,\middle|\, S\lambda_s\right\rangle \\ &\quad = \sqrt{3(2S+1)}W\left(2, 1, \frac{3}{2}, \frac{1}{2}; 1, S\right)\left\langle 2m_\ell S\lambda_s \,\middle|\, \frac{3}{2}\lambda_\Delta\right\rangle \\ &\quad = -(-1)^{1/2-S}\frac{1}{\sqrt{2}}\left\langle 2m_\ell S\lambda_s \,\middle|\, \frac{3}{2}\lambda_\Delta\right\rangle, \end{aligned} \tag{A15}$$

giving Eq. (2.37).

APPENDIX B: INTEGRATION IN k

When the currents associated to the Δ D-states are written there is a dependence in the tensor

$$I^{\alpha\beta}(P_+, P_-) = \int_k \mathcal{D}^{\alpha\beta}(P_+, k)\psi^{D2S}_\Delta(P_+, k)\psi^S_N(P_-, k). \tag{B1}$$

The properties of $I^{\alpha\beta}$ in a Lorentz transformation follows the properties of $\mathcal{D}^{\alpha\beta}$

$$\mathcal{D}^{\alpha\beta}(P'_+, k') = \Lambda^\alpha_\sigma\Lambda^\beta_\rho\mathcal{D}^{\sigma\rho}(P_+, k). \tag{B2}$$

Then

$$I^{\alpha\beta}(P'_+, P'_-) = \Lambda^\alpha_\sigma\Lambda^\beta_\rho I^{\sigma\rho}(P_+, P_-). \tag{B3}$$

In these conditions, a covariant expression for $I^{\alpha\beta}(P_+, P_-)$ can be derived in a particular frame and the extended for an arbitrary frame using (B3).

Consider Eq. (B1) in the Δ rest frame. In the Δ rest frame the scalar wave functions are independent of the variable φ. In these conditions, we can perform the analytical integration in φ, replacing the integral expression, by a equivalent integral with an integrand function independent of φ. The result is

$$\frac{1}{2\pi}\int d\varphi \mathcal{D}^{\alpha\beta}(P_+, k) = S_3 \bar{R}^{\alpha\beta}, \tag{B4}$$

where $z = \cos\theta$ (θ is the angle between $\mathbf{k}$ and $\mathbf{q}$) and

$$S_3 = \frac{\mathbf{k}^2}{2}(1 - 3z^2), \tag{B5}$$

$$\bar{R}^{\alpha\beta} = \begin{bmatrix} 0 & 0 & 0 & 0 \\ 0 & 1/3 & 0 & 0 \\ 0 & 0 & 1/3 & 0 \\ 0 & 0 & 0 & -2/3 \end{bmatrix}. \tag{B6}$$

We can express (B4) in a covariant form considering covariant expressions for S_3 and $\bar{R}^{\alpha\beta}$

$$S_3 \to b(k, q) \qquad \bar{R}^{\alpha\beta} \to R^{\alpha\beta}(P_+, P_-).$$

In particular, we can write in the Δ rest frame

$$b(\tilde{k}, \tilde{q}) = \frac{3}{2}\frac{(\tilde{k}\cdot\tilde{q})^2}{\tilde{q}^2} - \frac{1}{2}\tilde{k}^2, \tag{B7}$$

$$R^{\alpha\beta}(P_+, P_-) = \frac{\tilde{q}^\alpha \tilde{q}^\beta}{\tilde{q}^2} - \frac{1}{3}\tilde{g}^{\alpha\beta}. \tag{B8}$$

The expression $R^{\alpha\beta}(P_+, P_-)$ is the only covariant expression for $\bar{R}^{\alpha\beta}$ compatible with (B6), as can be showed considering the most general expression

$$R^{\alpha\beta}(P_+, P_-) = \frac{a}{M^2}P_+^\alpha P_+^\beta + \frac{b}{M^2}P_+^\alpha P_-^\beta + \frac{c}{M^2}P_-^\alpha P_+^\beta + \frac{d}{M^2}P_-^\alpha P_-^\beta + e g^{\alpha\beta}, \tag{B9}$$

where a, b, c, d, and e are functions of Q^2.

Similarly, the identity (B7) is the only possible covariant representation of S_3. Equivalent representation involving the factors $\tilde{q}\cdot k$ or $q\cdot\tilde{k}$ are reduced to $\tilde{q}\cdot\tilde{k}$. By definition of $\tilde{k}$ and $\tilde{q}$, $\tilde{k}\cdot q = \tilde{q}\cdot k = \tilde{q}\cdot\tilde{k}$.

As consequence of the representation (B7) and (B8), the integral (B4) in the Δ rest frame can be represented by

$$\frac{1}{2\pi}\int d\varphi \mathcal{D}^{\alpha\beta}(P_+, k) = b(\tilde{k}, \tilde{q}) R^{\alpha\beta}(P_+, P_-). \tag{B10}$$

As (B10) is expressed in a covariant notation we can obtain the equivalent expression for a different collinear frame considering an appropriate boost.

Using Eq. (B10) we can write for any collinear frame

$$I^{\alpha\beta}(P_+, P_-) = R^{\alpha\beta}(P_+, P_-) I_D(P_+, P_-), \tag{B11}$$

where

$$I_D(P_+, P_-) = \int_k b(\tilde{k}, \tilde{q})\psi_\Delta^{D2S}(P_+, k)\psi_N^S(P_-, k). \tag{B12}$$

[1] M. K. Jones *et al.* (Jefferson Lab Hall A Collaboration), Phys. Rev. Lett. **84**, 1398 (2000).
[2] O. Gayou *et al.* (Jefferson Lab Hall A Collaboration), Phys. Rev. Lett. **88**, 092301 (2002).
[3] V. Punjabi *et al.*, Phys. Rev. C **71**, 055202 (2005); **71**, 069902(E) (2005).
[4] F. Gross, G. Ramalho, and M. T. Pena, Phys. Rev. C **77**, 015202 (2008).
[5] F. Gross, G. Ramalho, and M. T. Pena, Phys. Rev. C **77**, 035203 (2008).
[6] F. Gross and P. Agbakpe, Phys. Rev. C **73**, 015203 (2006).
[7] C. E. Hyde-Wright and K. de Jager, Annu. Rev. Nucl. Part. Sci. **54**, 217 (2004).
[8] J. Arrington, C. D. Roberts, and J. M. Zanotti, J. Phys. G **34**, S23 (2007).
[9] C. F. Perdrisat, V. Punjabi, and M. Vanderhaeghen, Prog. Part. Nucl. Phys. **59**, 694 (2007).
[10] R. Beck *et al.*, Phys. Rev. C **61**, 035204 (2000); T. Pospischil *et al.*, Phys. Rev. Lett. **86**, 2959 (2001); D. Elsner *et al.*, Eur. Phys. J. A **27**, 91 (2006); N. F. Sparveris *et al.*, Phys. Lett. B **651**, 102 (2007).
[11] S. Stave *et al.*, Eur. Phys. J. A **30**, 471 (2006).
[12] G. Blanpied *et al.*, Phys. Rev. C **64**, 025203 (2001); Phys. Rev. Lett. **79**, 4337 (1997).
[13] C. Mertz *et al.*, Phys. Rev. Lett. **86**, 2963 (2001); N. F. Sparveris *et al.* (OOPS Collaboration), Phys. Rev. Lett. **94**, 022003 (2005).
[14] V. V. Frolov *et al.*, Phys. Rev. Lett. **82**, 45 (1999); K. Joo *et al.* (CLAS Collaboration), Phys. Rev. Lett. **88**, 122001 (2002).
[15] M. Ungaro *et al.* (CLAS Collaboration), Phys. Rev. Lett. **97**, 112003 (2006).
[16] C. E. Carlson, Phys. Rev. D **34**, 2704 (1986); C. E. Carlson and N. C. Mukhopadhyay, Phys. Rev. Lett. **81**, 2646 (1998); C. E. Carlson, arXiv:hep-ph/9809595.
[17] G. Sterman and P. Stoler, Annu. Rev. Nucl. Part. Sci. **47**, 193 (1997).
[18] A. M. Bernstein, Eur. Phys. J. A **17**, 349 (2003).
[19] A. M. Bernstein and C. N. Papanicolas, AIP Conf. Proc. **904**, 1 (2007).
[20] V. Pascalutsa and M. Vanderhaeghen, Phys. Rev. D **73**, 034003 (2006).

[21] T. A. Gail and T. R. Hemmert, Eur. Phys. J. A **28**, 91 (2006).
[22] C. Fernandez-Ramirez, E. Moya de Guerra, and J. M. Udias, Phys. Rev. C **73**, 042201(R) (2006).
[23] D. Arndt and B. C. Tiburzi, Phys. Rev. D **69**, 014501 (2004); **68**, 114503 (2003); **69**, 059904(E) (2004).
[24] V. Pascalutsa and M. Vanderhaeghen, Phys. Rev. D **76**, 111501 (2007).
[25] C. A. Dominguez and R. Rontsch, J. High Energy Phys. 10 (2007) 085.
[26] A. Idilbi, X. Ji, and J. P. Ma, Phys. Rev. D **69**, 014006 (2004).
[27] M. M. Giannini, AIP Conf. Proc. **904**, 179 (2007).
[28] N. Isgur, G. Karl, and R. Koniuk, Phys. Rev. D **25**, 2394 (1982).
[29] S. Capstick and B. D. Keister, Phys. Rev. D **51**, 3598 (1995).
[30] S. Capstick and G. Karl, Phys. Rev. D **41**, 2767 (1990).
[31] S. Capstick, Phys. Rev. D **46**, 2864 (1992).
[32] B. Julia-Diaz, D. O. Riska, and F. Coester, Phys. Rev. C **69**, 035212 (2004); B. Julia-Diaz and D. O. Riska, Nucl. Phys. **A757**, 441 (2005).
[33] M. De Sanctis, M. M. Giannini, E. Santopinto, and A. Vassallo, Eur. Phys. J. A **19**, 81 (2004).
[34] J. F. Donoghue, E. Golowich, and B. R. Holstein, Phys. Rev. D **12**, 2875 (1975).
[35] M. Warns, W. Pfeil, and H. Rollnik, Phys. Rev. D **42**, 2215 (1990).
[36] R. Bijker, F. Iachello, and A. Leviatan, Ann. Phys. (N.Y.) **236**, 69 (1994).
[37] Y. B. Dong, Phys. Lett. B **638**, 333 (2006).
[38] J. Yu, T. Wang, C. R. Ji, and B. Q. Ma, Phys. Rev. D **76**, 074009 (2007).
[39] V. Keiner, Z. Phys. A **359**, 91 (1997).
[40] M. Gorchtein, D. Drechsel, M. M. Giannini, E. Santopinto, and L. Tiator, Phys. Rev. C **70**, 055202 (2004).
[41] T. Sato and T. S. H. Lee, Phys. Rev. C **54**, 2660 (1996); **63**, 055201 (2001).
[42] B. Julia-Diaz, T. S. Lee, A. Matsuyama, T. Sato, and L. C. Smith, Phys. Rev. C **77**, 045205 (2008); **76**, 065201 (2007); A. Matsuyama, T. Sato, and T. S. Lee, Phys. Rep. **439**, 193 (2007).
[43] B. Julia-Diaz, T. S. H. Lee, T. Sato, and L. C. Smith, Phys. Rev. C **75**, 015205 (2007).
[44] S. S. Kamalov and S. N. Yang, Phys. Rev. Lett. **83**, 4494 (1999).
[45] S. S. Kamalov, S. N. Yang, D. Drechsel, O. Hanstein, and L. Tiator, Phys. Rev. C **64**, 032201(R) (2001).
[46] G. L. Caia, L. E. Wright, and V. Pascalutsa, Phys. Rev. C **72**, 035203 (2005); G. L. Caia, V. Pascalutsa, J. A. Tjon, and L. E. Wright, Phys. Rev. C **70**, 032201(R) (2004); V. Pascalutsa and J. A. Tjon, Phys. Rev. C **70**, 035209 (2004).
[47] G. Kalbermann and J. M. Eisenberg, Phys. Rev. D **28**, 71 (1983).
[48] M. Fiolhais, B. Golli, and S. Sirca, arXiv:hep-ph/9512391.
[49] L. Amoreira, P. Alberto, and M. Fiolhais, Phys. Rev. C **62**, 045202 (2000).
[50] K. Bermuth, D. Drechsel, L. Tiator, and J. B. Seaborn, Phys. Rev. D **37**, 89 (1988).
[51] D. H. Lu, A. W. Thomas, and A. G. Williams, Phys. Rev. C **55**, 3108 (1997).
[52] A. Faessler, T. Gutsche, B. R. Holstein, V. E. Lyubovitskij, D. Nicmorus, and K. Pumsa-ard, Phys. Rev. D **74**, 074010 (2006); arXiv:hep-ph/0612246.
[53] A. J. Buchmann, E. Hernandez, and A. Faessler, Phys. Rev. C **55**, 448 (1997); A. J. Buchmann, E. Hernandez, U. Meyer, and A. Faessler, Phys. Rev. C **58**, 2478 (1998); U. Meyer, E. Hernandez, and A. J. Buchmann, Phys. Rev. C **64**, 035203 (2001).
[54] Q. B. Li and D. O. Riska, Nucl. Phys. A **766**, 172 (2006); Phys. Rev. C **73**, 035201 (2006).
[55] G. Vereshkov and N. Volchanskiy, Phys. Rev. D **76**, 073007 (2007).
[56] V. M. Braun, A. Lenz, and M. Wittmann, Phys. Rev. D **73**, 094019 (2006); V. M. Braun, A. Lenz, G. Peters, and A. V. Radyushkin, Phys. Rev. D **73**, 034020 (2006).
[57] J. Rohrwild, Phys. Rev. D **75**, 074025 (2007).
[58] P. Stoler, Phys. Rev. D **65**, 053013 (2002); Phys. Rev. Lett. **91**, 172303 (2003); P. Stoler, arXiv:hep-ph/0307162.
[59] V. Pascalutsa, C. E. Carlson, and M. Vanderhaeghen, Phys. Rev. Lett. **96**, 012301 (2006).
[60] C. E. Carlson and M. Vanderhaeghen, Phys. Rev. Lett. **100**, 032004 (2008).
[61] D. B. Leinweber, T. Draper, and R. M. Woloshyn, Phys. Rev. D **48**, 2230 (1993).
[62] C. Alexandrou, Ph. de Forcrand, H. Neff, J. W. Negele, W. Schroers, and A. Tsapalis, Phys. Rev. Lett. **94**, 021601 (2005).
[63] C. Alexandrou *et al.*, Phys. Rev. D **69**, 114506 (2004).
[64] C. Alexandrou, G. Koutsou, H. Neff, J. W. Negele, W. Schroers, and A. Tsapalis, Phys. Rev. D **77**, 085012 (2008).
[65] V. Pascalutsa, M. Vanderhaeghen, and S. N. Yang, Phys. Rep. **437**, 125 (2007).
[66] V. D. Burkert and T. S. H. Lee, Int. J. Mod. Phys. E **13**, 1035 (2004).
[67] S. Stave *et al.* (A1 Collaboration), Phys. Rev. C **78**, 025209 (2008).
[68] G. Ramalho, M. T. Pena, and F. Gross, Eur. Phys. J. A **36**, 329 (2008).
[69] T. S. Lee, JLAB Report No. JLAB-THY-07-757.
[70] A. J. Buchmann and E. M. Henley, Phys. Rev. C **63**, 015202 (2000).
[71] A. J. Buchmann, Phys. Rev. Lett. **93**, 212301 (2004).
[72] A. J. Buchmann, AIP Conf. Proc. **904**, 110 (2007).
[73] D. Drechsel and L. Tiator, AIP Conf. Proc. **904**, 129 (2007).
[74] L. Tiator and S. Kamalov, AIP Conf. Proc. **904**, 191 (2007).
[75] D. Drechsel, S. S. Kamalov, and L. Tiator, Eur. Phys. J. A **34**, 69 (2007).
[76] D. Drechsel, O. Hanstein, S. S. Kamalov, and L. Tiator, Nucl. Phys. A **645**, 145 (1999).
[77] MAID website, http://www.kph.unimainz.de.
[78] R. A. Arndt, I. I. Strakovsky, R. L. Workman, and M. M. Pavan, Phys. Rev. C **52**, 2120 (1995).
[79] R. A. Arndt, I. I. Strakovsky, and R. L. Workman, Phys. Rev. C **53**, 430 (1996).
[80] R. A. Arndt, I. I. Strakovsky, and R. L. Workman, Int. J. Mod. Phys. A **18**, 449 (2003).
[81] SAID website, http://gwdac.phys.gwu.edu.
[82] I. G. Aznauryan, Phys. Rev. C **68**, 065204 (2003).

[83] I. G. Aznauryan, Phys. Rev. C **67**, 015209 (2003).
[84] L. C. Smith (CLAS Collaboration), AIP Conf. Proc. **904**, 222 (2007).
[85] F. Gross, Phys. Rev. **186**, 1448 (1969).
[86] F. Gross, J. W. Van Orden, and K. Holinde, Phys. Rev. C **45**, 2094 (1992).
[87] F. Gross and Y. Surya, Phys. Rev. C **47**, 703 (1993); Y. Surya and F. Gross, Phys. Rev. C **53**, 2422 (1996).
[88] W. Rarita and J. S. Schwinger, Phys. Rev. **60**, 61 (1941).
[89] F. J. Milford Phys. Rev. **98**, 1488 (1955).
[90] M. Benmerrouche, R. M. Davidson, and N. C. Mukhopadhyay, Phys. Rev. C **39**, 2339 (1989).
[91] H. Haberzettl, arXiv:nucl-th/9812043.
[92] W. W. Buck and F. Gross, Phys. Rev. D **20**, 2361 (1979).
[93] H. F. Jones and M. D. Scadron, Ann. Phys. (N.Y.) **81**, 1 (1973).
[94] A. Stadler and F. Gross, Phys. Rev. Lett. **78**, 26 (1997).
[95] A. Stadler, F. Gross, and M. Frank, Phys. Rev. C **56**, 2396 (1997).
[96] F. Gross, A. Stadler, and M. T. Pena, Phys. Rev. C **69**, 034007 (2004).
[97] J. Adam, F. Gross, C. Savkli, and J. W. Van Orden, Phys. Rev. C **56**, 641 (1997).
[98] J. V. Noble, Phys. Rev. C **17**, 2151 (1978).
[99] U. G. Meissner, AIP Conf. Proc. **904**, 142 (2007).
[100] W. Bartel *et al.*, Phys. Lett. **28**, 148B (1968).
[101] S. Stein *et al.*, Phys. Rev. D **12**, 1884 (1975).
[102] R. A. Arndt, W. J. Briscoe, I. I. Strakovsky, and R. L. Workman, AIP Conf. Proc. **904**, 269 (2007).
[103] M. Vanderhaeghen, AIP Conf. Proc. **904**, 25 (2007).
[104] M. E. Rose, *Elementary Theory of Angular Momentum* (John Wiley & Sons, Inc., New York, 1957). See Equation (6.5a).